

AD-A054 987

IIT RESEARCH INST CHICAGO ILL
ELF ELECTRIC AND MAGNETIC FIELD SIMULATION FOR A LABORATORY BIO--ETC(U)
MAY 78 J R GAUGER

F/G 6/18

N00039-76-C-0141

NL

UNCLASSIFIED

IITRI-E6357-10

| OF |
AD
A054 987



END
DATE
FILED
7-78
DDC

ADA054987

FOR FURTHER TRAN

14
9 IITRI-
15 Technical Report E6357-10
Contract N00039-76-C-0141

12 IITRI

16 ELF ELECTRIC AND MAGNETIC FIELD SIMULATION
FOR A LABORATORY BIOLOGICAL EXPERIMENT.

10 J. R. /Gauger

11 May 78

12 59 P.

AD No. _____
DDC FILE COPY

Prepared for:

U.S. Naval Electronics Systems Command
Washington, D.C.

Submitted by:

IIT Research Institute
10 West 35th Street
Chicago, Illinois 60616

DDC
RECORDED
RECEIVED
JUN 12 1978
A

DISTRIBUTION STATEMENT A
Approved for public release
Distribution Unlimited

175350

act

FOREWORD

This document was prepared for the Special Communications Project Office of the U. S. Naval Electronic Systems Command by IIT Research Institute under Contract N00039-76-C-0141.

The technical report herein describes an extremely low frequency (ELF) electromagnetic (EM) field simulator which was designed and built in support of biological tissue culture experiments performed at the Naval Medical Research Institute, Bethesda, Maryland. The simulator generates uniform electric and magnetic fields having the same characteristics as those which would be produced by the U. S. Navy's proposed ELF communications system. A companion report "ELF Electric Field Analysis for a Laboratory Biological Experiment", IITRI Technical Report E6357-9, covers an analysis of the electric field levels induced in individual tissue culture samples when exposed to electromagnetic fields in the laboratory simulator.

The electric and mechanical design, checkout, installation, and field mapping of the simulator were the responsibility of Mr. J. Gauger. Mr. W. Lancaster did the mechanical fabrication and electrical wiring, and aided in the installation and field mapping.

Respectfully submitted,

IIT RESEARCH INSTITUTE

J. R. Gauger
J. R. Gauger
Associate Engineer

APPROVED

R. D. Carlson
R. D. Carlson
Program Manager

A. R. Valentino
A. R. Valentino, Manager
EM Effects Section

ACCESSION NO.		White Section <input checked="" type="checkbox"/>
B&G		Buff Section <input type="checkbox"/>
ORIGINATOR		
INSTITUTION		
DISTRIBUTION AVAILABILITY CODES		
DATE	AVAIL. END	SPECIAL
<i>A</i>		

IIT RESEARCH INSTITUTE

TABLE OF CONTENTS

	<u>Page</u>
FOREWORD	ii
1. INTRODUCTION	1
2. SIMULATOR DESIGN	5
2.1 Design Considerations and Specifications	5
2.2 Design Realization	6
2.2.1 Magnetic Field Coils and Electric Field Plates . .	6
2.2.2 Simulator Drive and Control Circuitry	13
3. SIMULATOR INSTALLATION AND CHECKOUT	26
3.1 Exposure Room Layout and Simulator Installation	26
3.2 Electromagnetic Field Measurements	29
3.2.1 Equipment and Methods	29
3.2.2 Generated Field Inside the Incubator	31
3.2.3 60 Hz Ambient Fields	31
3.2.4 Cross-Coupling of Simulator Generated Fields . . .	36
3.2.5 Simulator Generated External Fields	36
REFERENCES	42
APPENDIX A. Design of a Multi-Coil Magnetic Field Simulator	43

LIST OF TABLES AND FIGURES

Table

		<u>Page</u>
1	Simulator Generated 76 Hz Electric Field Intensity (E) and Magnetic Flux Density (B) Inside Incubator "A"	33
2	60 Hz Ambient Electric Field Intensity and Magnetic Flux Density Inside Incubators A & B.	35
3	Simulator Cross-Coupling at 76 Hz.	37
4	76 Hz Simulator Generated Magnetic Flux Densities Outside the Incubators	38
5	60 Hz EM Fields Near Electrical Appliances/Devices	39
6	60 Hz EM Fields in the Center of Various Rooms in a Typical Home.	41
A-1	Listing of Fortran IV Computer Program to Calculate the Off-Axis B-Field Due to Multiple Coaxial Coils	48

Figure

1	ELF Electromagnetic Field Simulator.	2
2	Tissue Culture Growth Tray	3
3	Front View--ELF Electromagnetic Field Simulator Construction Details	10
4	Top View--Sect. A ELF Electromagnetic Field Simulator Construction Details	11
5	Simulator Support & Mounting Plate	12
6	Position of Culture Trays in the Simulator--Front View . . .	14
7	Position of Culture Trays in the Simulator--Top View--Section "A".	15
8	Block Diagram of the Simulator Drive and Control System. . .	16
9	Simulator Drive Circuitry Schematic Drawing.	17
10	Temporary Test Setup of the Electromagnetic Field Simulator Drive Circuitry.	18
11	Rear View of Simulator Control Panel and Chassis	20
12	Resistor and Capacitor Bank Chassis.	21
13	Buffer Amplifier Schematic Drawing	23
14	Simulator Interlock Controls Schematic Drawing	24
15	Layout of ELF Exposure, Room 115--NMRI	27
16	Incubator; ELF Electromagnetic Field Simulator Installation; and Simulated Control, Drive, and Monitoring Equipment . . .	28
17	Magnetic Field Probe and High Impedance Electric Field Probe with Plexiglass Stands	30

LIST OF TABLES AND FIGURES (Cont.)

<u>Figure</u>		<u>Page</u>
18	Test Point Numbering and Location with Respect to the Electric Field Plates	32
A-1	Cylindrical Coordinate System for a Circular Loop	47
A-2	Coordinate System for the Three Coil Configuration.	50
A-3	Comparison of the Measured and Calculated Magnetic Flux Density Along the Simulator Axis ($\rho = 0$).	52
A-4	Comparison of the Measured and Calculated Magnetic Flux Density versus Perpendicular Distance from the Simulator Axis at $z = 0$	53

1. INTRODUCTION

Modern technology has developed many applications for radio frequency and microwave electromagnetic energy. These applications include communications, remote detection, industrial processing, food preparation, and medical diagnosis and therapy. This extensive usage has led to concern about the potential for biological hazards from electromagnetic (EM) radiation exposure and to the setting of national standards for the maximum permissible exposure for humans.¹ The possible effects on organisms of extremely low frequency (ELF, 20 to 100 Hz) electric and magnetic fields are also being studied. This research includes the Navy's proposed ELF Communications System^{2,3} as well as power systems.⁴ The research spans a broad spectrum of biological sciences, from enzymes to mammalian behavior, and from bacteria and slime molds to primates.

Recently, research has been initiated at the Naval Medical Research Institute (NMRI) to study the possible effects of the electric and magnetic fields associated with the Navy's proposed ELF Communications System (Seafarer) on human tissue cultures. The necessary electrical engineering support for this experiment is provided by the IIT Research Institute (IITRI). Two ELF electromagnetic field simulators were designed and built by IITRI for the NMRI experiments. They employ parallel metallic plates to generate a uniform electric field and a multiple coil configuration to generate a uniform magnetic field. A photograph of one of the simulators is shown in Figure 1. For the experiments, the simulators were placed inside incubators, which were necessary to maintain the proper conditions for growth of the tissues. Plastic, many-celled trays, such as the one shown in Figure 2, were used to contain the tissue cultures. The trays were placed on stands between the plates of the ELF EM simulators.

The purpose of this report is to present the details of the design and fabrication of the ELF electromagnetic field simulators at IITRI and the installation of the simulators and the measuring of their generated EM fields at NMRI. These topics are discussed in Sections 2 and 3, respectively.

In the test volume of the simulator, both electric and magnetic fields are induced inside the biological tissue. The important aspect of the present problem of electromagnetic coupling and interaction is the determination of

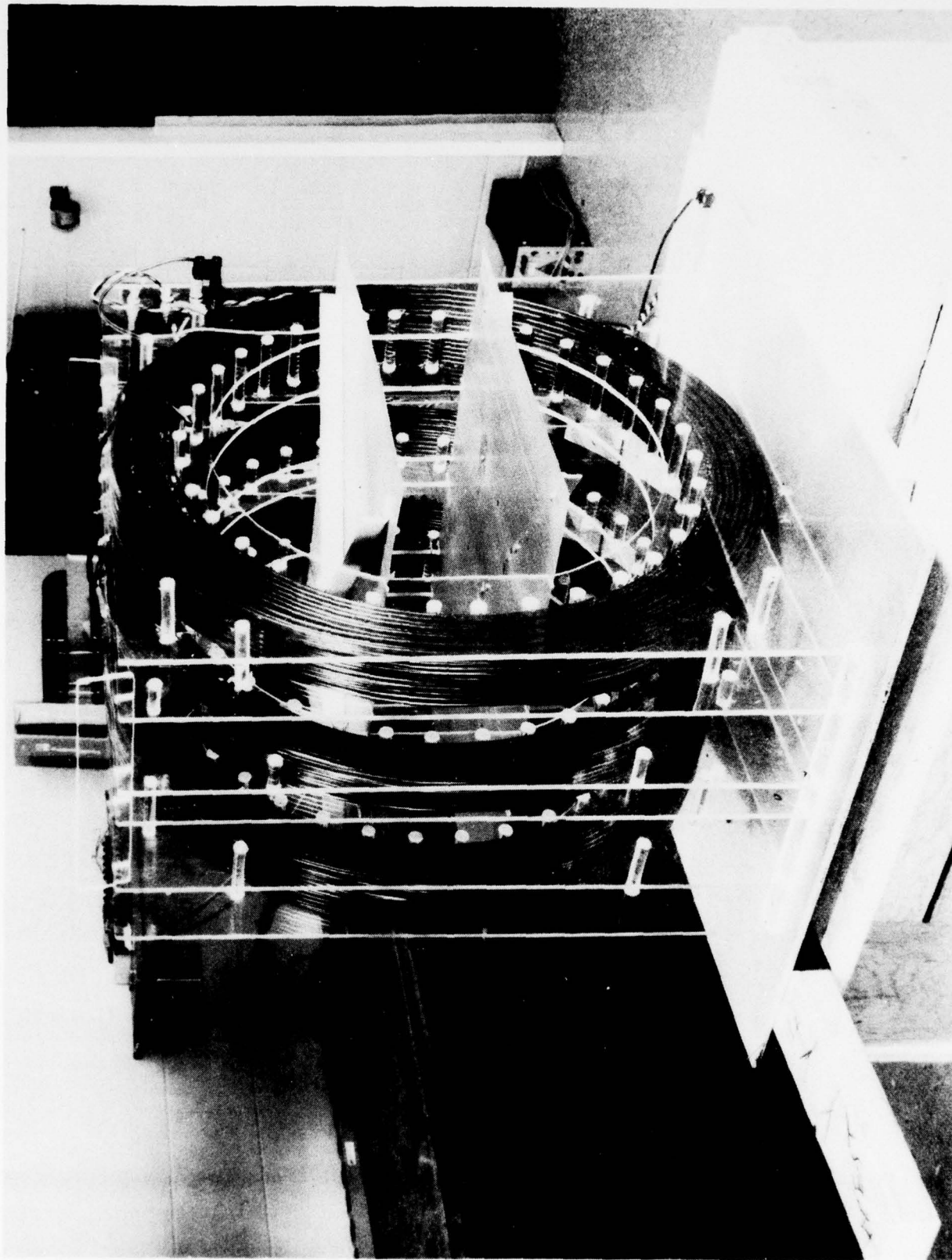


Figure 1 ELF ELECTROMAGNETIC FIELD SIMULATOR



Figure 2 TISSUE CULTURE GROWTH TRAY

the electric field strength and the magnetic field strength induced inside the tissue culture. For the case of present interest, the magnetic field inside the tissue culture has a magnitude equal to that of the impressed field, and suffers no significant distortion because the frequency of interest is low and the permeabilities of the biological tissue and their surrounding medium are essentially that of free space. Determination of the electric field strength internal to the biological tissue must be done either by experimental measurement or by theoretical analysis. It is difficult to accurately measure the internal electric field strength because of the fact that the electric field strength internal to a very high permittivity object is low, and because the test specimens are small. Thus, the electric field coupled into the biological tissue in the plastic tray of Figure 2 was determined analytically. A companion report⁵ presents the details of this analysis.

2. SIMULATOR DESIGN

2.1 Design Considerations and Specifications

The design of an ELF electromagnetic field simulator to be used as the stress in a biological experiment employing tissue cultures required consideration of a number of potential problems. These could be grouped into three main areas:

1. physical and environmental restrictions imposed by the tissue culture, their life support equipment, and the servicing of both;
2. specification of the type of electrical signal and the electromagnetic field levels to be generated; and
3. requirements concerning the monitoring of critical system parameters and avoidance of worker exposure to the stress EM fields.

The growth of tissue culture in a laboratory necessitates a strictly controlled environment, usually provided by means of an incubator. This allows maintenance of the proper temperature (in this case, 37°C), elevated humidity, a carbon dioxide enriched atmosphere, and essentially sterile conditions. Tissue cultures are often grown in partitioned plastic trays, such as the type shown in Figure 2, which were used in this experiment. The environmental requirements just discussed define a number of design criteria for the electromagnetic field simulator:

1. the simulator must fit inside the incubator and be adequately supported;
2. materials must be used which are corrosion resistant and which do not support bacterial or fungal growth;
3. heat generated by the simulator must not disrupt the temperature equilibrium of the incubator;
4. access to the humidity bath must be provided for cleaning and refilling;
5. the simulator must allow adequate air circulation within the incubator to maintain a uniform environment;
6. provision must be made for support of the tissue culture trays within the simulator.

The design parameters for the electrical aspects of the simulator were determined primarily by the characteristics of the signal and the electromagnetic fields of the Seafarer ELF communications system and by the electromagnetic field levels specified by the experimental protocol. The ELF signal to be used to drive the simulator is called an MSK, or minimum shift keying, signal. It is basically a type of frequency modulation (FM) in which the signal shifts back and forth between two frequencies, called the mark and space frequencies, at a given rate called the modulation frequency. The specific frequencies used for this system are a mark frequency (f_h) of 80 Hz, a space frequency (f_l) of 72 Hz, a center frequency (or average of f_h and f_l , f_o) of 76 Hz, and a modulation frequency (f_c) of 16 Hz.

In order to accurately simulate the electromagnetic fields of the ELF communications system, the simulator had to generate electric and magnetic fields which were perpendicular to one another in the test volume. In addition, the electrical signals driving the electric and magnetic fields were required to be 90° out of phase. The requirements of the experimental protocol necessitated that the simulator be able to generate magnetic field levels from 0 to 10 gauss, and electric field levels from 0 to 200 volts/meter.

Monitoring of system parameters was necessary to assure that any discontinuities which occurred during the experiments would be detected, and also assure that the test and control setups were as closely matched as possible. Due to the sensitivity of the tissue cultures to temperature, this parameter had to be measured to 0.5°C resolution, and continuously monitored. The electric and magnetic field levels had to be monitored to assure proper operating conditions and to detect any failure of the field generating apparatus. It was also desired to detect any intermittent power failure or unauthorized opening of an incubator door, and to interrupt the electric and magnetic fields when the test incubator door was opened.

2.2 Design Realization

2.2.1 Magnetic Field Coils and Electric Field Plates

The design of an electromagnetic field simulator may be separated, to some extent, into the design of an electric field simulator and the design of a magnetic field simulator. Design of a simulator to generate a uniform

electric field over a given volume is fairly simple and straightforward. Parallel metallic plates are used to generate an electric field between and perpendicular to the metallic plates. The width and depth of the plates should be at least three times the separation of the plates to minimize distortion and fringing of the electric field near the plate edges. In general, it is also desirable to keep the plate separation at least three times greater than the thickness of the object to be placed between the plates. When used in conjunction with a magnetic field simulator, the electric field plates must be placed within the magnetic field generating structure so the magnetic field simulator will not distort the electric field between the plates. Thus, the size of the magnetic field simulator determines the maximum size of the plates of the electric field simulator.

The design of a magnetic field simulator generally follows one of two configurations: a set of Helmholtz coils or a solenoidal coil. These configurations are popular because the fields along their main axes are easily determined. The solenoidal coil has the desired uniform field over most of its internal volume, but the closed tubular nature of its construction does not permit the proper circulation of air among tissue cultures located inside of it. Further, solenoidal coils capable of producing uniform magnetic fields must be long in comparison with their diameter. This severely limits the size of electric field plates which could be placed inside a solenoidal if the solenoid length was limited.

A coaxial pair of simple Helmholtz coils with radii equal to the coil separation can be shown to produce an especially uniform magnetic field near the axis. However, in order to determine how large the coils would have to be to obtain the desired field uniformity within the required test volume, the variation of the field away from the axis must be known. As the expressions for determining the off-axis fields were not readily available in the literature, a theoretical analysis was performed to determine the quasi-static magnetic field at any point in space due to any number of coaxial circular coils. This analysis is described in considerable detail in Appendix A.

Based on the theoretical analysis, a multi-coil configuration which optimizes magnetic field uniformity over the coil volume was determined.

The configuration is basically a pair of Helmholtz coils with a third coil added between them. The middle coil has only half as many turns as the end coils but carries the same current. Using the classical expression for the magnetic field on the axis of a circular current loop⁶ and the superposition theorem, the expression for the total magnetic flux density on the main axis at the center coil for a three coil simulator can be derived as:

$$B_{\text{total}} = \frac{\mu_0 N I R^2}{2} \left(\frac{1}{R^3} + 2 \cdot \frac{2}{(R^2 + X^2)^{3/2}} \right) \times 10^4 \quad (1)$$

where

B_{total} = the magnetic flux density in gauss

μ_0 = the permeability of free space, $4\pi \times 10^{-7}$ henry/meter

N = the number of turns on the middle coil (end coils have $2N$ turns)

I = the rms value of the coils in amperes

R = the mean radius of the coils in meters

X = the coil separation, $R/2$, in meters.

The approximate dimensions of the incubator changes in which the simulators were to be contained were: 27 inches high by 27 inches wide by 26 inches deep. Based on these dimensions, a maximum coil diameter of 26 inches was chosen, for a nominal mean radius (R) of 12 inches and a nominal coil separation (X) of 6 inches. Using these values of X and R in Equation 1, along with a maximum value of 10 gauss for B_{total} as previously stated, a turns-current product was defined:

$$NI = 124 \quad (2)$$

The values of N and I are dependent on the maximum power to be dissipated in the coils as heat, and on the maximum voltage drop to appear across the coils. The nominal rating of the heating element in the incubator was 80 watts. Therefore, so as not to upset the critical temperature equilibrium of the chamber, the dissipation of the coils was limited to five percent of the heater rating, or four watts. To minimize generation of an electric field by the magnetic field coils, the voltage drop across the coils should

be as small as possible. This indicated a coil with few turns for low inductance and large wire diameter for low resistance. To satisfy these requirements, N was chosen as 50 turns and I as 2.48 amperes. The wire gauge was nominally 6 AWG, consisting of 27 strands of 20 AWG copper wire. This yielded a total coil dissipation of 3.7 watts, a resistance 0.602 ohm, and an approximate inductance of 25 mH.

Figures 3 and 4 are front and top section views, respectively, of the mechanical details of the electromagnetic field simulator. The magnetic field coils were wound ten layers deep on plexiglass forms created by spacing quarter-inch thick square plates with half-inch diameter rods. The center of the plexiglass forms was cut out to allow room for the electric field plates and for air circulation. The electric field plates, which were cut from perforated stainless steel sheet and reinforced with fiberglass angles, rested in slits cut in the side of the coil forms. In keeping with the minimum width to separation ratio of 3:1, the plates measured 18 by 24 inches with a 6-inch spacing. Plexiglass spacers were used to keep the three coils at the proper separation. A photograph of the assembled electromagnetic field simulator was shown in Figure 1.

In order to support the considerable weight of the three magnetic field coils, about 180 pounds,* a special one-fourth inch thick aluminum base plate was fabricated, as shown in Figure 5. This plate was substituted for a much thinner plate used in the incubator for channeling air over the humidity bath at the bottom of the chamber. The heavier mounting plate, in addition to supporting and positioning the coils, also served to duct air over the bath. It had legs made of aluminum rod along one edge of the plate instead of a solid rail support, to permit air flow under the plate. Access to the humidity bath for cleaning and filling was provided through a notch cut in the left front corner of the plate. The cutout was covered with a removable panel.

* It can be shown that for a given magnetic field strength, coil size, and coil power dissipation, the weight of the copper in the coil windings is essentially constant-- independent of the wire gauge and number of turns.

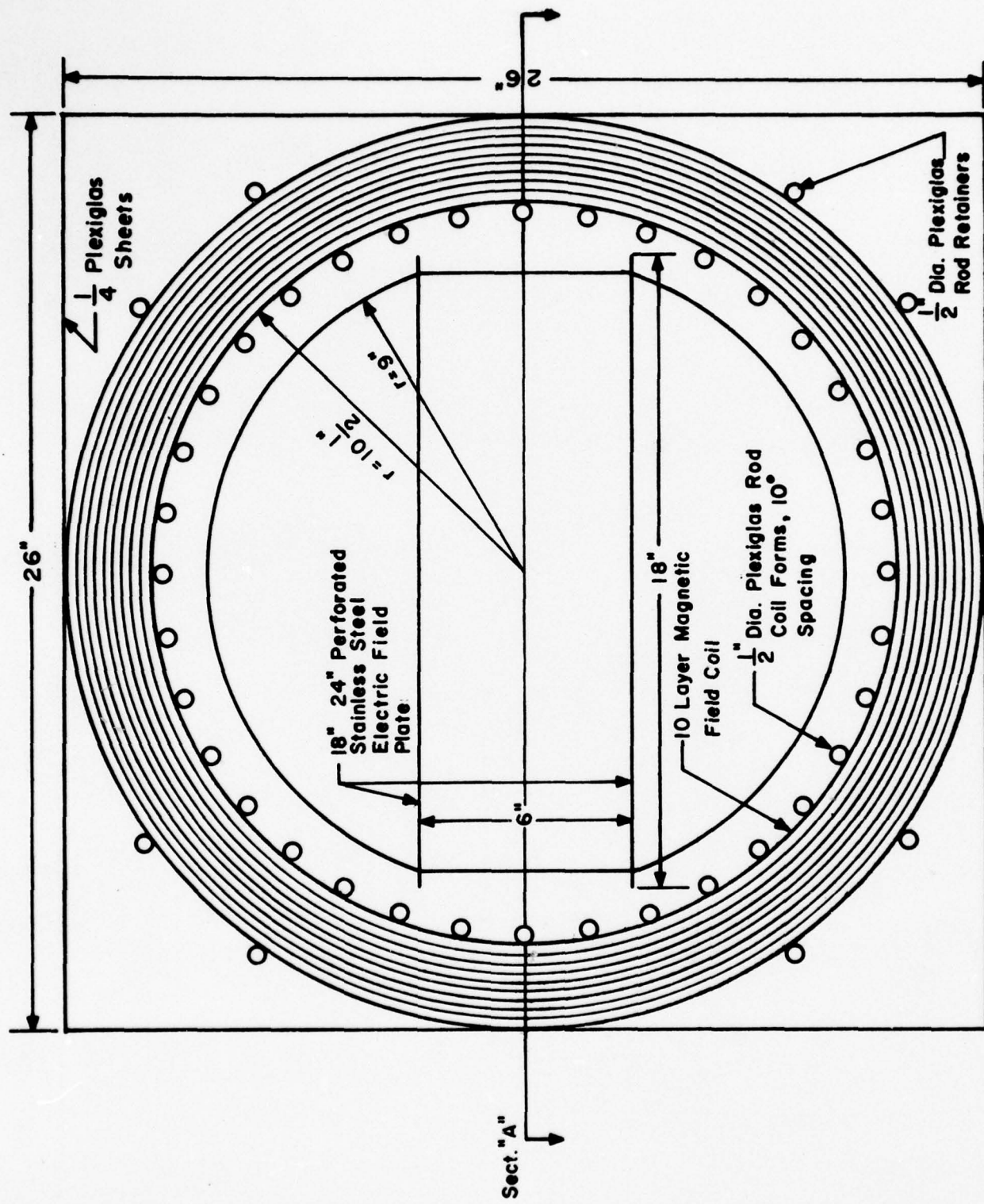


Fig. 3

FRONT VIEW- ELF ELECTROMAGNETIC FIELD SIMULATOR CONSTRUCTION DETAILS

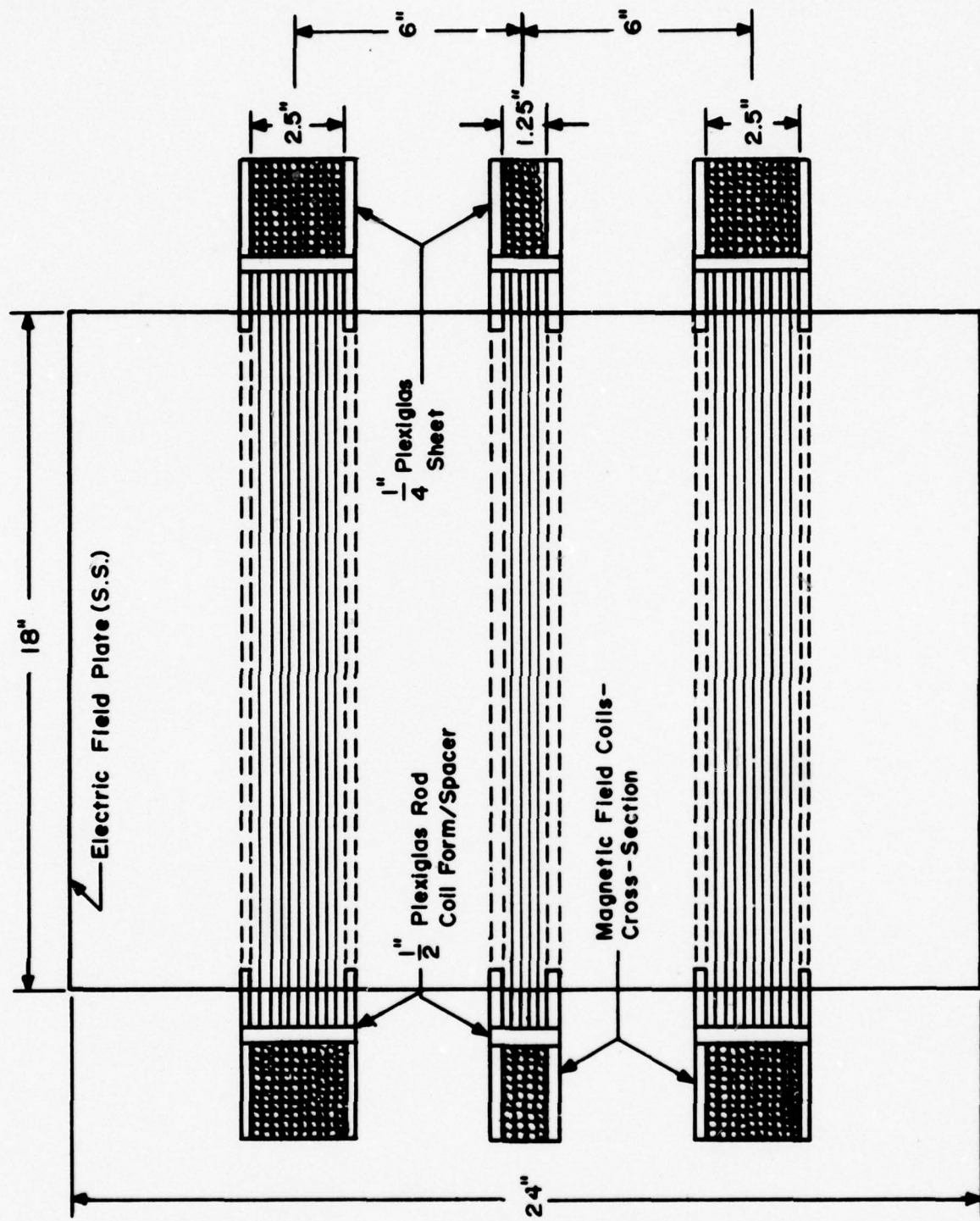


Fig. 4
TOP VIEW - SECT.A ELF ELECTROMAGNETIC FIELD SIMULATOR
CONSTRUCTION DETAILS

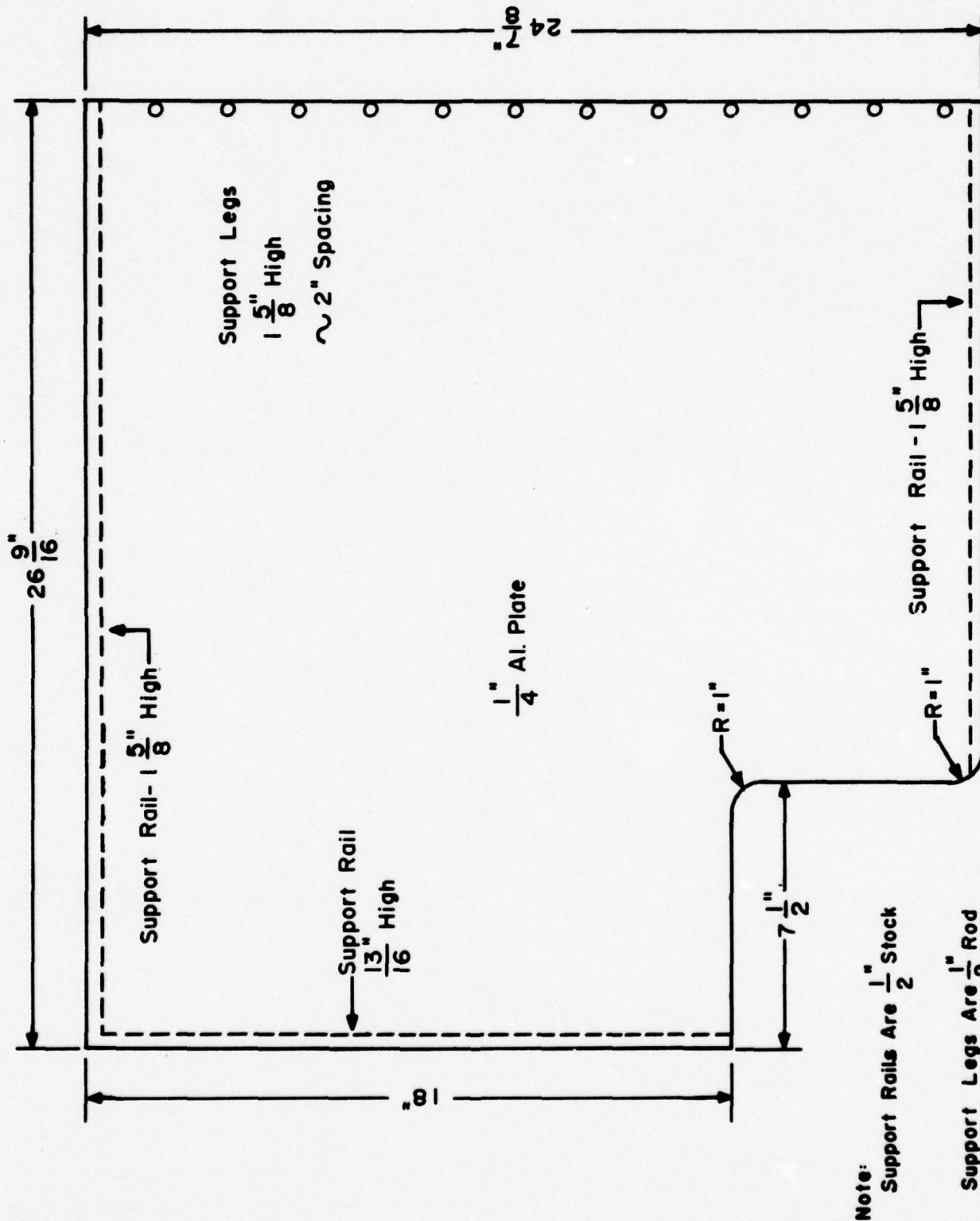


Fig. 5
SIMULATOR SUPPORT & MOUNTING PLATE

Figures 6 and 7 show the location of the tissue culture trays within the electromagnetic field simulator. The trays were situated four to a level, and from one to five levels high. Plexiglass tables were used to support the trays midway between the electric field plates; tables with different heights were used for each number of layers. The dimensions of the electric field plates were roughly three times those of the tissue culture trays, as desired, to ensure a uniform electric field over the test volume. Likewise, the trays were also centered in the magnetic field coils where the magnetic field is most uniform. Note that the electric and magnetic fields generated by the simulator were perpendicular to one another as required. The magnetic field inside the coils was horizontal, parallel to the main axis of the coils; the electric field generated by the metallic plates was oriented vertically.

2.2.2 Simulator Drive and Control Circuitry

A block diagram of the simulator drive and control circuitry is presented in Figure 8. The main components of the system are an MSK signal source, an audio power amplifier, a control panel and drive circuitry, the electric field plates and magnetic field coils, and field monitoring equipment. A schematic diagram of the drive circuitry for the electromagnetic field simulator is given in Figure 9. A photograph of the equipments associated with the block diagram is shown in Figure 10. Note the temporary use of an Elgar 1001 power source in place of the Crown D-150A power amplifier (bottom of figure).

The signal source was the IITRI designed and fabricated MSK signal generator.⁷ Two of the generators are mounted in the top of the equipment rack pictured in Figure 9. The generator is capable of producing the MSK signal with a center frequency 76 Hz, and mark the space frequencies of 80 and 72 Hz, respectively. The modulation of the signal is pseudo-random at a rate of 16 Hz. A second generator was dedicated to the system to provide an immediately available backup in case of a generator failure.

Amplification of the MSK signal and the necessary power to drive the simulator coils and plates was provided by a Crown D-150A audio power amplifier. This amplifier features very low distortion and high reliability -- necessary characteristics for a carefully controlled, long-term experiment. Reliability was enhanced further by the choice of this power amplifier as it has a factor of 2.5 reserve power margin at the maximum field level required.

IIT RESEARCH INSTITUTE

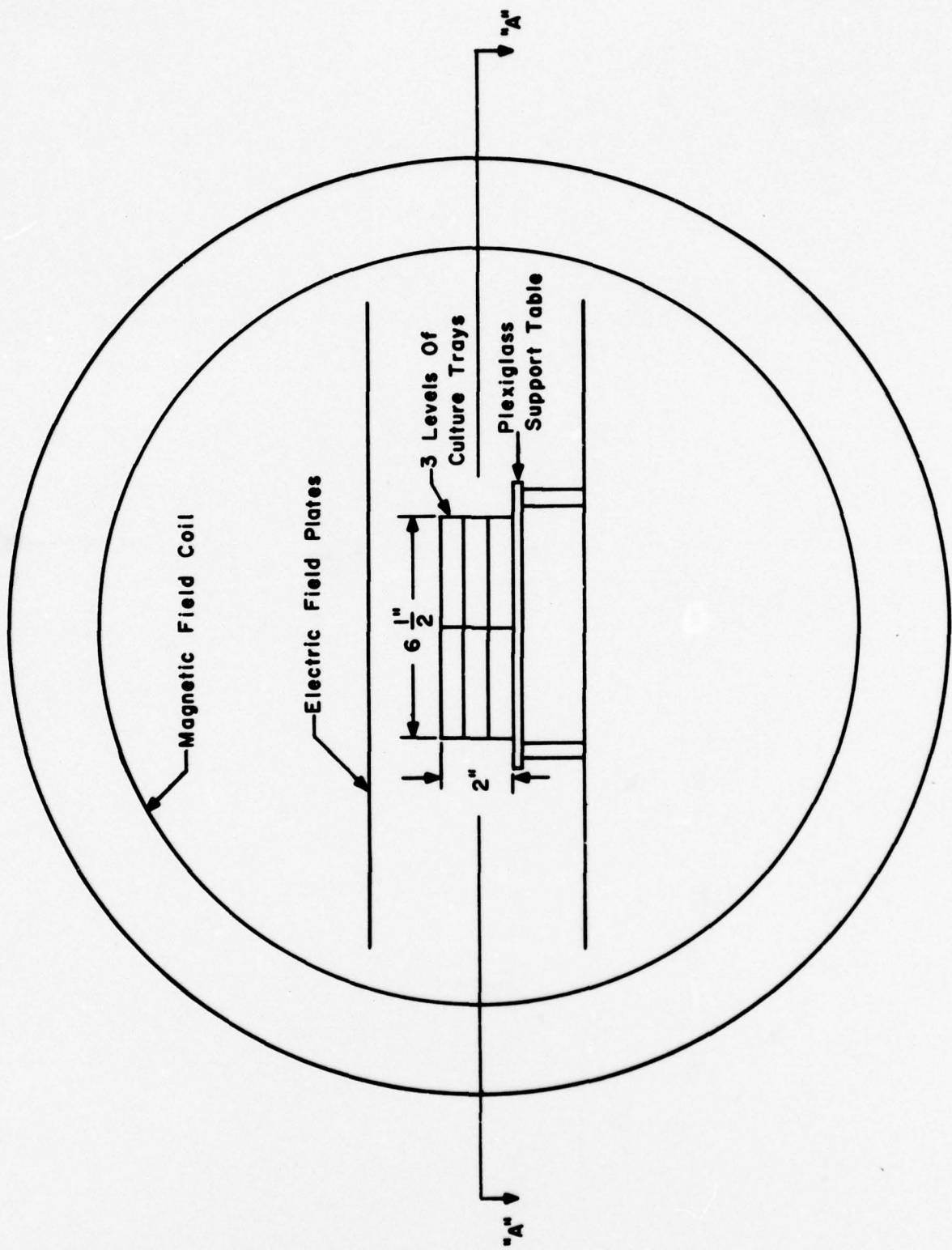


Fig. 6
POSITION OF CULTURE TRAYS IN THE SIMULATOR - FRONT VIEW

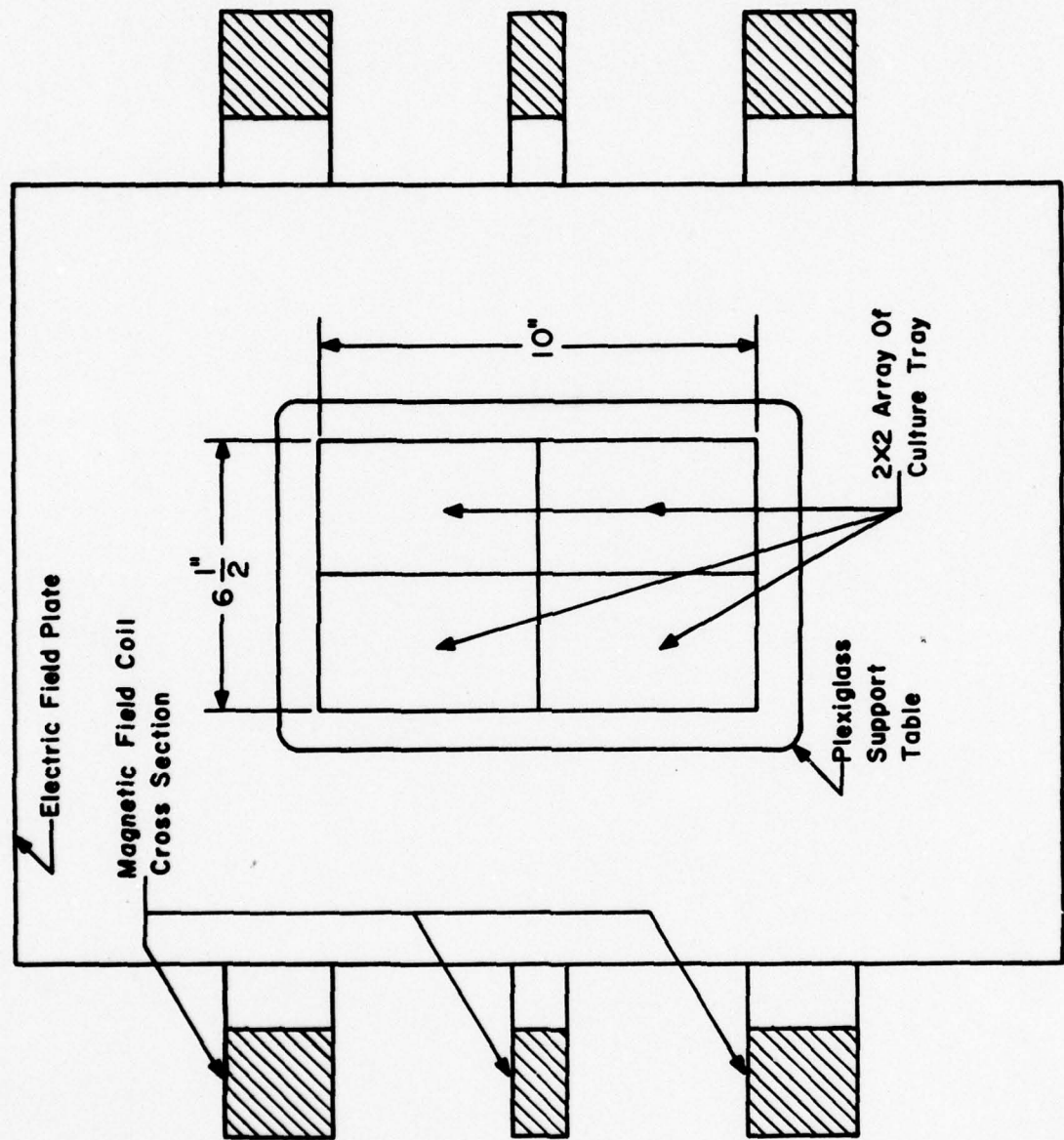


Fig. 7
POSITION OF CULTURE TRAYS IN THE SIMULATOR
TOP VIEW - SECTION "A"

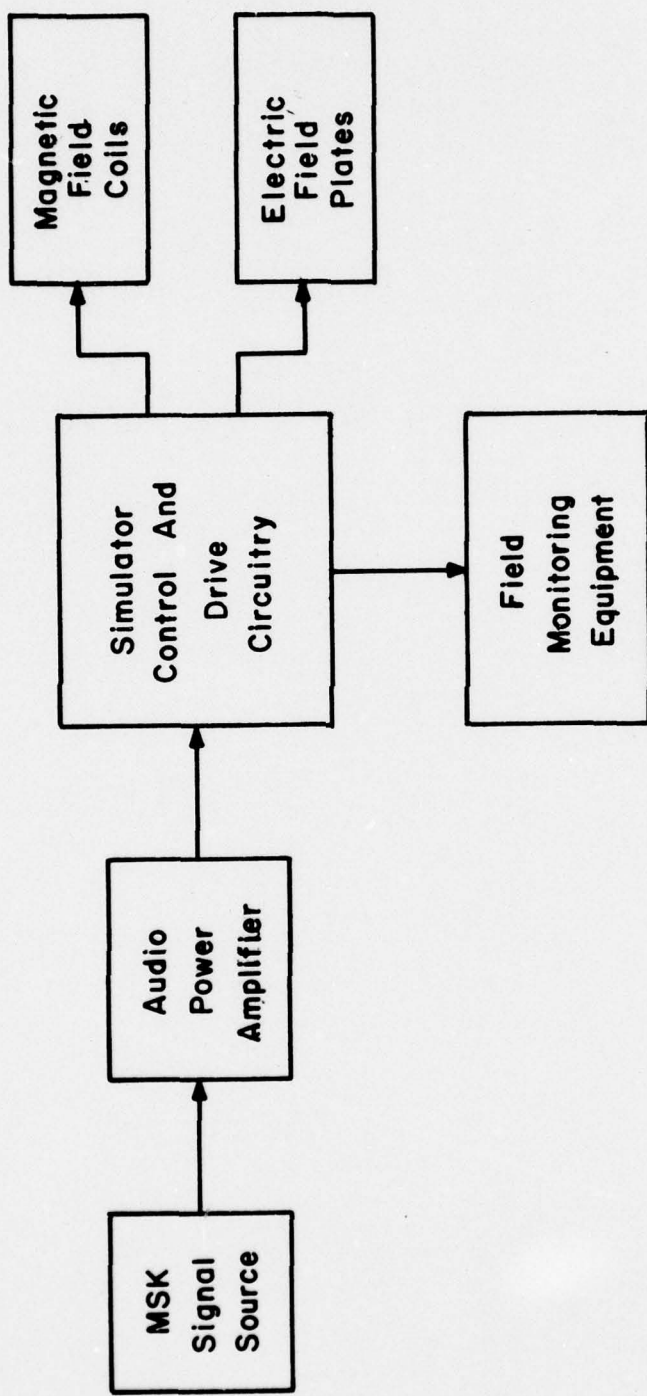
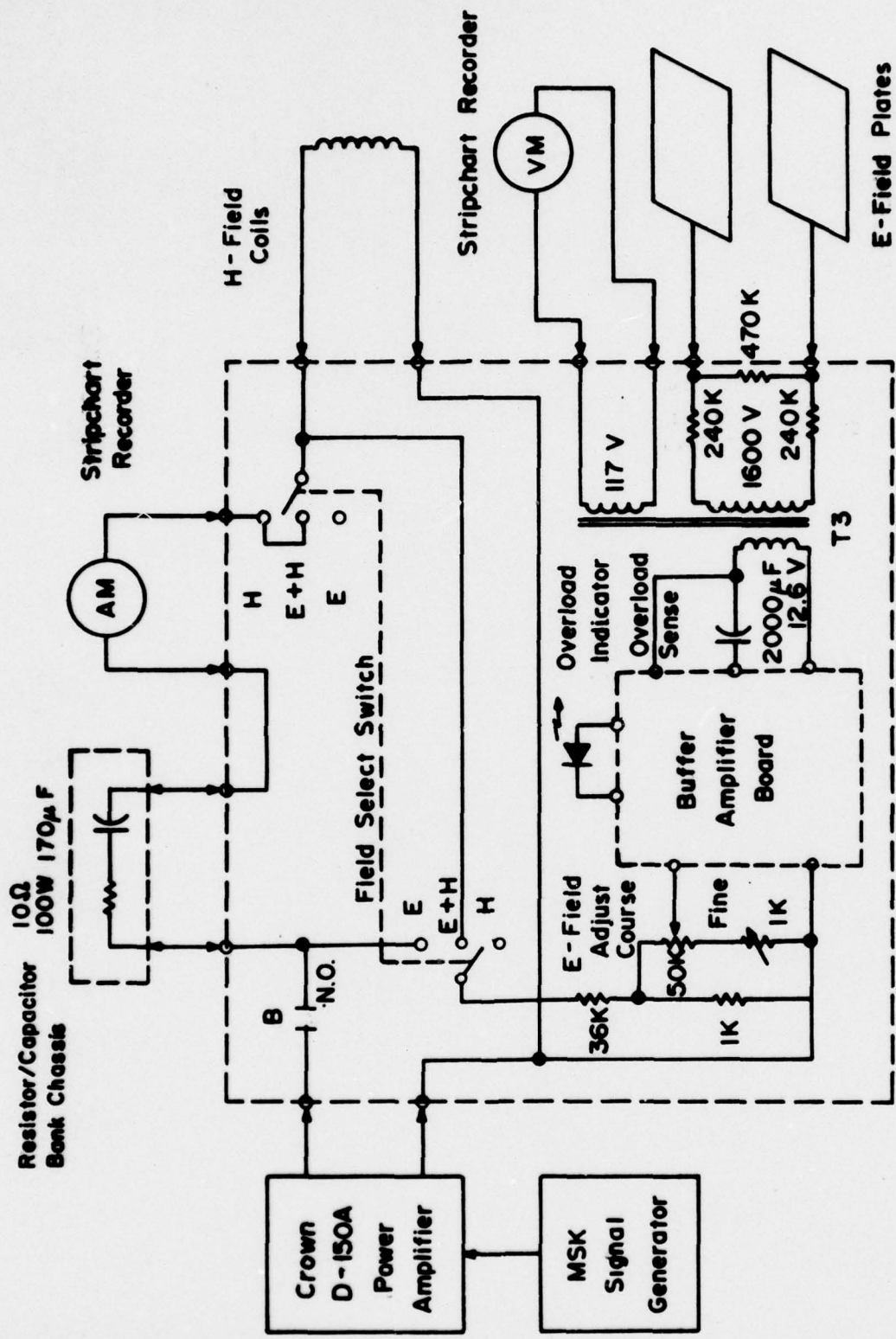


Fig. 8
BLOCK DIAGRAM OF THE SIMULATOR DRIVE AND CONTROL SYSTEM



Control Panel And Chassis

PROJECT NO.	Drawing No.	117 RESEARCH INSTITUTE
E6357		10 W. 35th Street Chicago, Illinois 60616
Scale None	Date Drawn 12/2/77	Figure 9 SIMULATOR DRIVE CIRCUITRY SCHEMATIC DRAWING

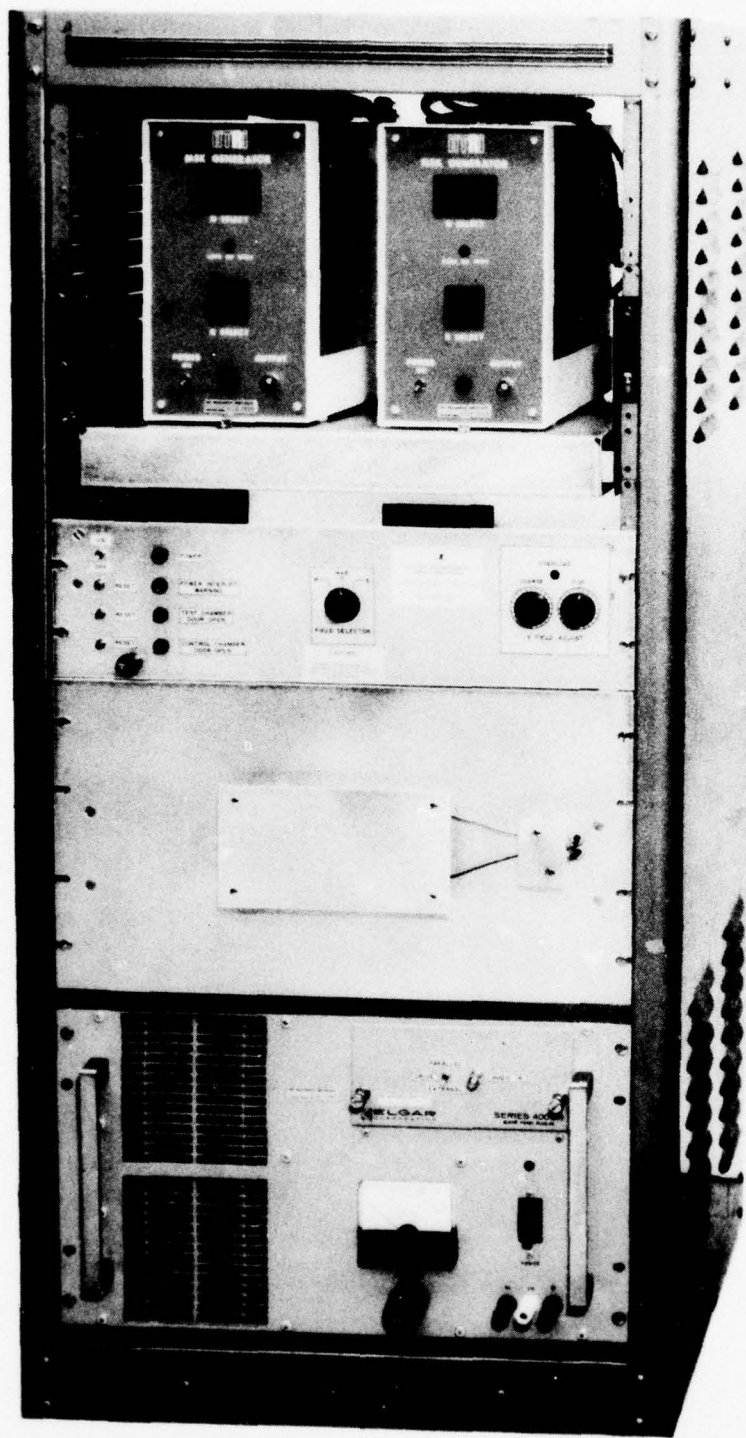


Figure 10 TEMPORARY TEST SETUP OF THE ELECTROMAGNETIC FIELD SIMULATOR DRIVE CIRCUITRY

The circuitry enclosed within the large area bounded by dashed lines in Figure 9 is located on the control panel and chassis assembly. The panel can be seen directly below the MSK generators in Figure 10, and a rear view of the panel and chassis is presented in Figure 11. Relay contact "B" shown within the area is an interlock controlled by the door of the test incubator. Thus, an open test chamber door or a power failure on the control chassis disconnects the drive amplifier from the rest of the drive circuitry. The usual operating mode of the simulator is simultaneous generation of electric and magnetic fields. To increase the simulator's flexibility, however, the ability to generate only one field at a time is provided via a field selector switch on the control panel.

The magnetic field coils are part of a series RLC circuit consisting of the coils, a 170 μ F capacitor bank, and a 10-ohm, 100-watt resistor. Due to their size, the resistor and capacitors are mounted on a separate chassis. The front of the chassis is shown in Figure 10 just below the control chassis. A rear view is given in the photograph in Figure 12. The resistor is mounted on the front panel, which also serves as a heat sink. A protective plate covers the resistor to eliminate any shock or burn hazard. The coils and the capacitor bank are tuned to the center frequency of the MSK signal, 76 Hz. At the MSK signal mark and space frequencies of 80 Hz and 72 Hz, the impedances of the LC network formed by the coils and capacitors are nominally 1 ohm inductive and 1 ohm capacitive, respectively. The values of these impedances are matched to within about five percent. The addition of the 10-ohm resistor detunes the series RLC network so that the change in the magnitude of the series impedance from 72 Hz to 80 Hz is only about 0.5 percent. This also allows the drive amplifier to be terminated with an essentially constant value and predominantly resistive load of the proper impedance. As the magnetic field generated by the coils is directly related to the coil current, a constant amplifier load, and hence a constant coil current, results in a magnetic field with the same amplitude at both 72 and 80 Hz.

The signal used to drive the electric field plates is the voltage which appears across the magnetic field coils. As the current and voltage in an inductor are known to be 90 degrees out of phase, the magnetic field, which is in phase with the coil current, is 90 degrees out of phase with the electric field. This is the desired relationship for simulation of the MSK ELF

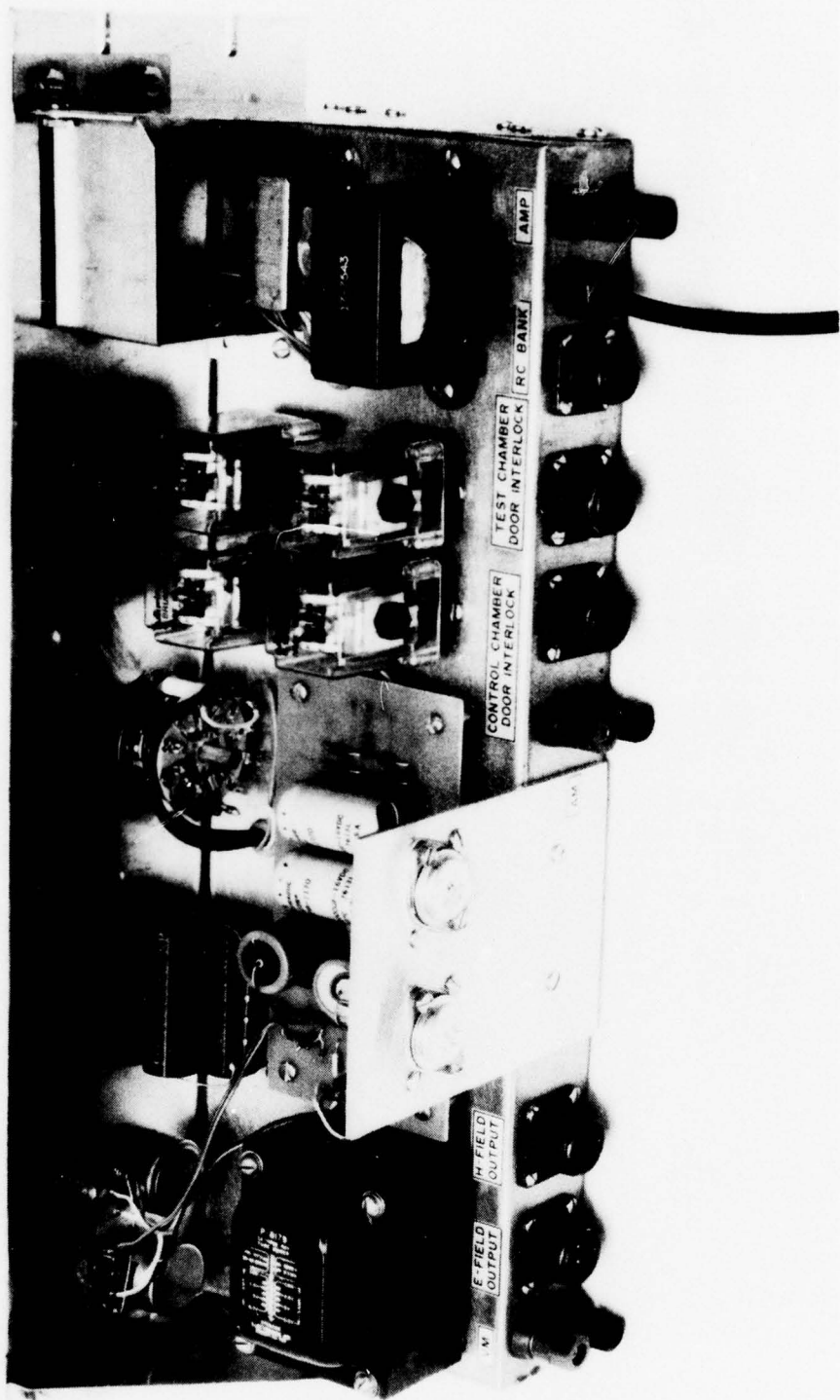


Figure 11 REAR VIEW OF SIMULATOR CONTROL PANEL AND CHASSIS

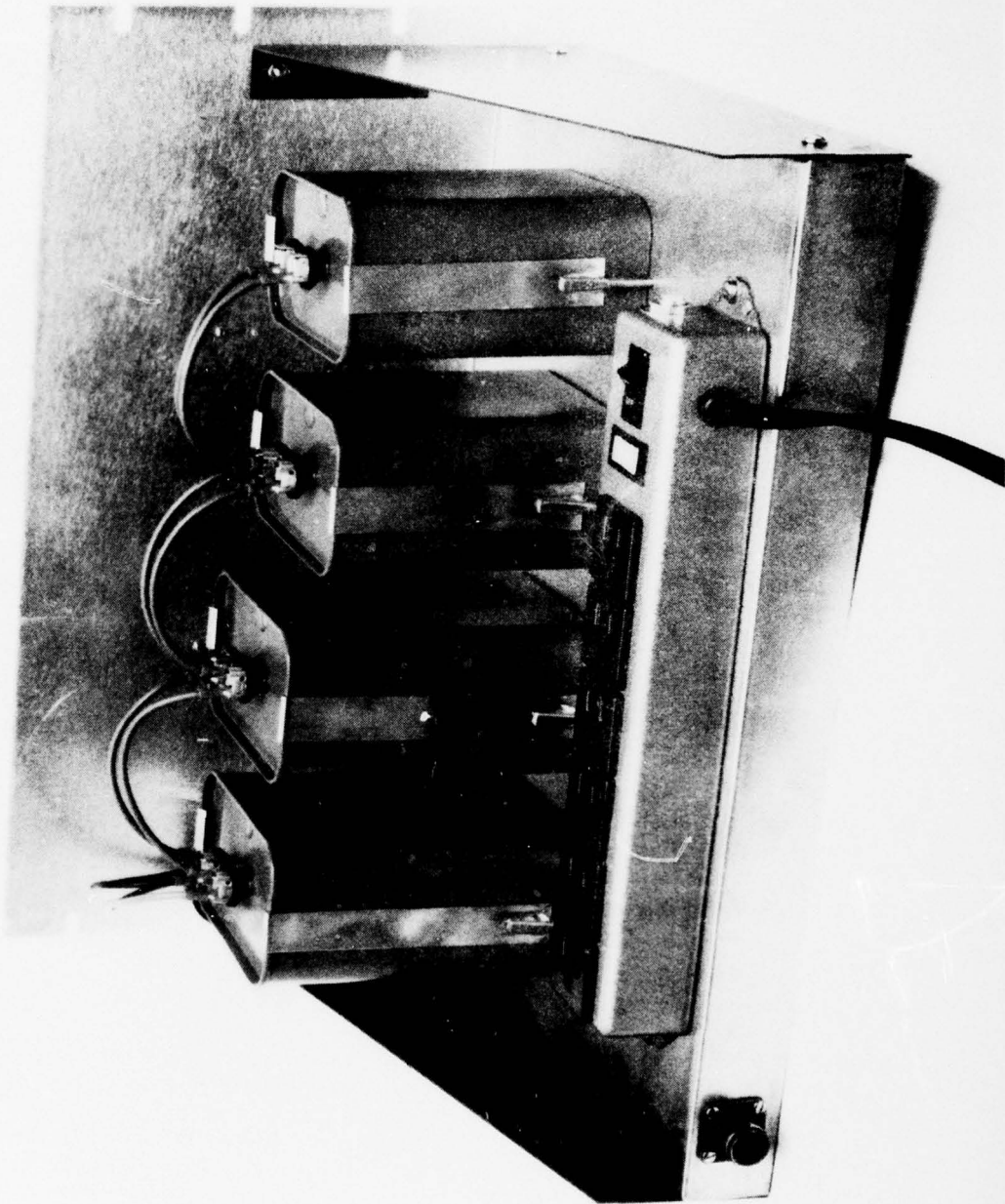
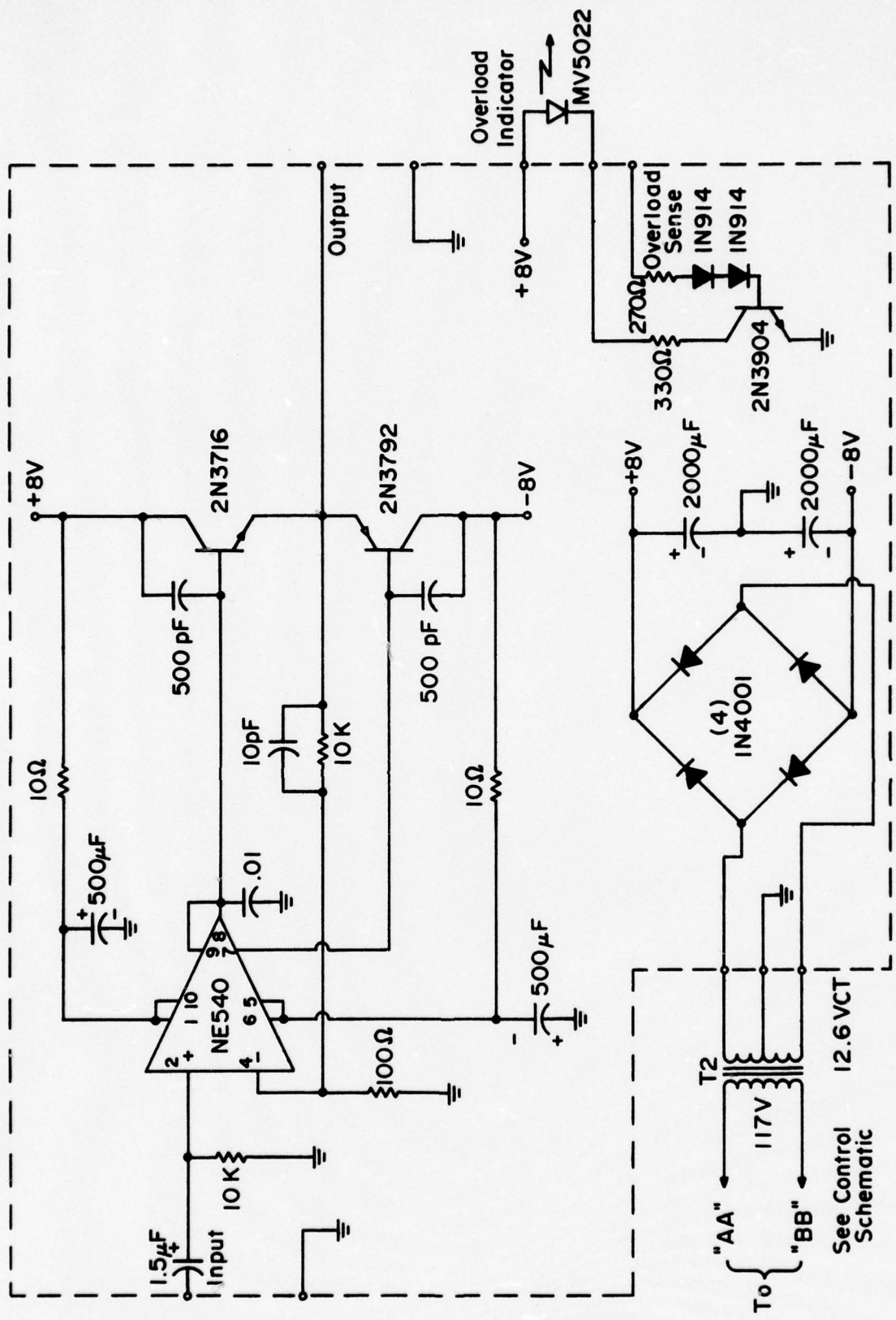


Figure 12 RESISTOR AND CAPACITOR BANK CHASSIS

electromagnetic fields of the proposed communications system. The actual phase angle will be slightly less than 90 degrees due to the finite Q (resistive loss) of the coils.

The drive circuit for the electric field plates as shown in Figure 9 consists of a variable input attenuator, a buffer amplifier, and a step-up transformer. The variable attenuator has both coarse and fine adjustments to provide the full range of electric field values over the full range of magnetic field levels. These adjustments are located on the control panel. The buffer amplifier has a high input impedance to minimize loading of the attenuator, and has a low output impedance to drive the transformer. The transformer output provides electrical isolation of the electric field plates, and provides the necessary plate voltages without the need for special high voltage power supplies. Series resistors on the transformer output limit the available short circuit source current of the electric field plates to less than 0.5 mA for the safety of operating personnel. An overload light senses the transformer primary voltage and indicates the maximum allowable level to avoid clipping and distortion of the electric field waveform. A schematic diagram of the buffer amplifier circuit is presented in Figure 13.

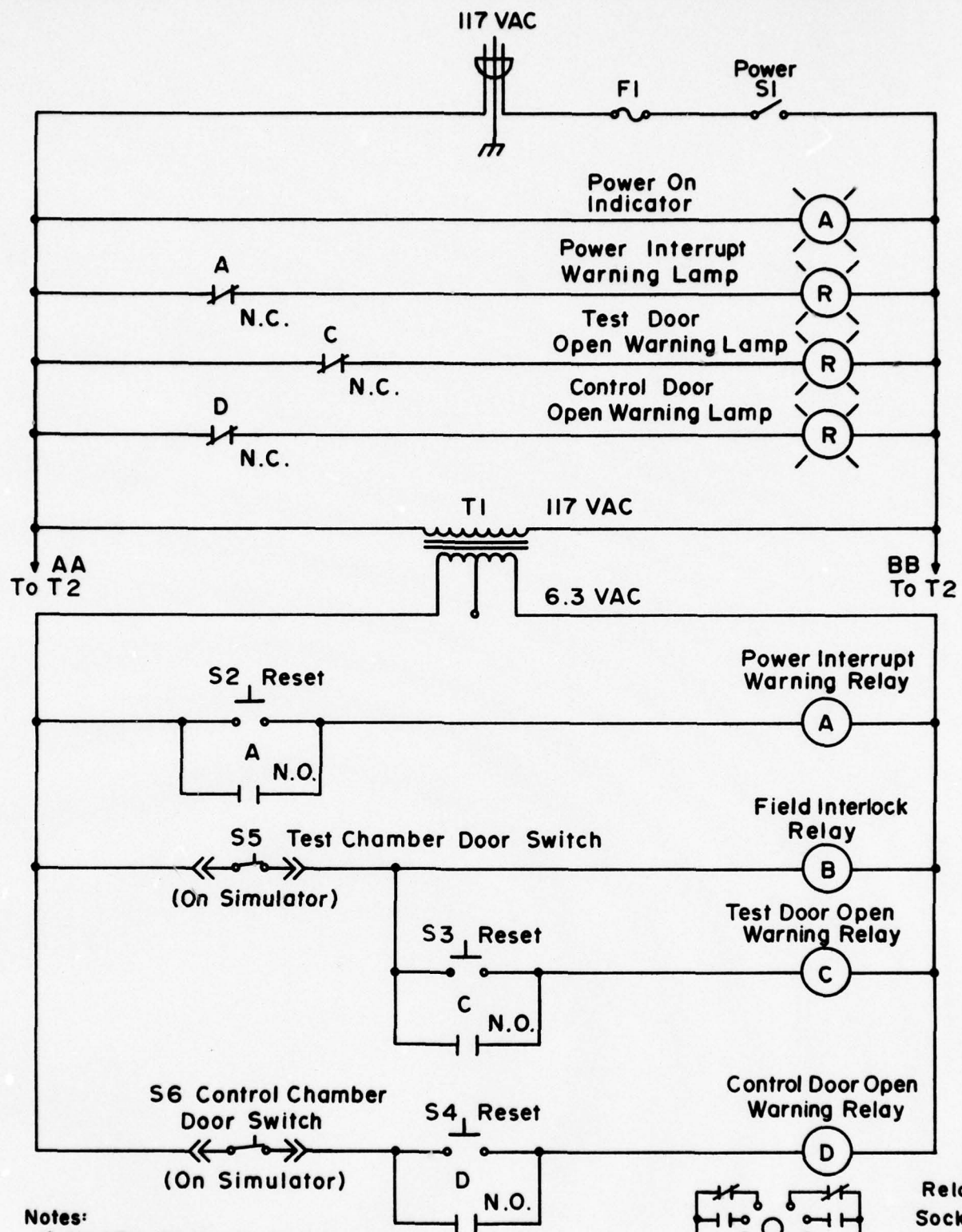
A schematic diagram of the simulator's interlock control circuitry is given in Figure 14. This circuitry is also located on the simulator control panel and chassis. Four indicator lamps are provided. The "power on" indicator gives the status of power switch S1. Switch S1 controls power to the interlock circuitry and to the buffer amplifier of Figure 12, and through field interlock relay "B" disconnects the main drive amplifier. The "power interrupt warning" lamp latches on in the event of a power failure, and will remain on until manually reset by S2. The "test door open warning" and "control door open warning" lamps are controlled by micro switches S5 and S6 which are located on the test and control incubator doors, respectively. These lamps are latched on in the event that an incubator door is opened, and must be manually reset by S3 or S4, as required. The door open warning lamps will also be triggered by an intermittent power failure. Note that all voltages associated with the reset switches and the remote door switches and wiring are transformer isolated and are no more than 6.3 VAC.



Notes:

- 1) T1 is on the Control Chassis
- 2) The Overload Indicator is on the Control Panel

PROJECT NO.	DRAWING NO.	IIT RESEARCH INSTITUTE
E6357		10 W. 35th Street Chicago, Illinois 60616
Scale None	Date Drawn 12/2/77	Figure 13 BUFFER AMPLIFIER SCHEMATIC DRAWING



Notes:

- 1) All 117V Wiring In Yellow
- 2) 6.3V Control Wiring In Orange & Green
- 3) All Parts Are Located On The Control Chassis Or Panel Except As Noted

PROJECT NO. E6357	Drawing No.	IIT RESEARCH INSTITUTE 10 W. 35th Street Chicago, Illinois 60616
Scale None	Date Drawn 12/2/77	Figure 14 SIMULATOR INTERLOCK CONTROLS SCHEMATIC DRAWING

Continuous monitoring of the electric and magnetic field levels was achieved with two stripchart recorders. A recorder responsive to ac current was used to measure and monitor the magnetic field; a recorder responsive to ac voltage was used for the electric field. At low field levels the current and voltage were too low to be accurately measured by the recorders, and an auxiliary ac ammeter and an ac voltmeter were installed to facilitate measurement of these parameters. The recorders were still useful, however, for indications of gross field level changes which might occur during periods when the simulators were unattended.

Two additional stripchart recorders were employed in conjunction with thermocouple probes to measure and continuously record the temperature in the test and control incubators. As the required incubator temperature was 37°C, a temperature span for the recorders of 30°C to 45°C was chosen. Resolution of the recorders was better than 0.5°C. All of the recorders had one-inch/hour chart speed, twelve inches of visible chart length, and thirty day recording capability per roll of chart paper.

3. SIMULATOR INSTALLATION AND CHECKOUT

3.1 Exposure Room Layout and Simulator Installation

A floor plan of ELF exposure Room 115 at the Naval Medical Research Institute is given in Figure 15. The incubators which contained the electromagnetic field simulators were set on a counter along one long wall of the room, and were spaced as far apart as possible to minimize cross-coupling of the generated fields from the test to the control incubator. Either incubator could be used as the test or control unit. Figure 16a is a photograph of incubator A in place in Room 115. Note the CO₂ tanks for the incubators to the left, and the experiment hood to the right of the incubator. The photograph in Figure 16b illustrates the installation of an ELF EM simulator in an incubator. Note the heavy duty base plate of the simulator and the humidity bath access cover in the lower left corner of the plate. The incubators were double-walled stainless steel units, with glass inner doors and double-walled stainless steel outer doors.

The simulator control, drive, and monitoring equipments were mounted on an open frame, nineteen-inch relay rack located between the two incubators. Photographs of the equipment rack are presented in Figures 16c and 16d. Visible on the rack, from top down, are:

1. two MSK generators;
2. the amplifier cooling fans;
3. the Crown D150A drive amplifier;
4. the field level and incubator temperature stripchart recorders;
5. the simulator control panel and chassis;
6. the resistor and capacitor bank chassis.

The drive cable from the instrument rack to the EM field simulators are electrically shielded and are routed behind the incubators and other equipment. The cable access to the simulators is made via a one-inch port in the upper front corner of the right side of the incubators. The door interlock switches are mounted on brackets on the inside of the outer incubator doors, and are actuated whenever the doors are opened more than about ten degrees.

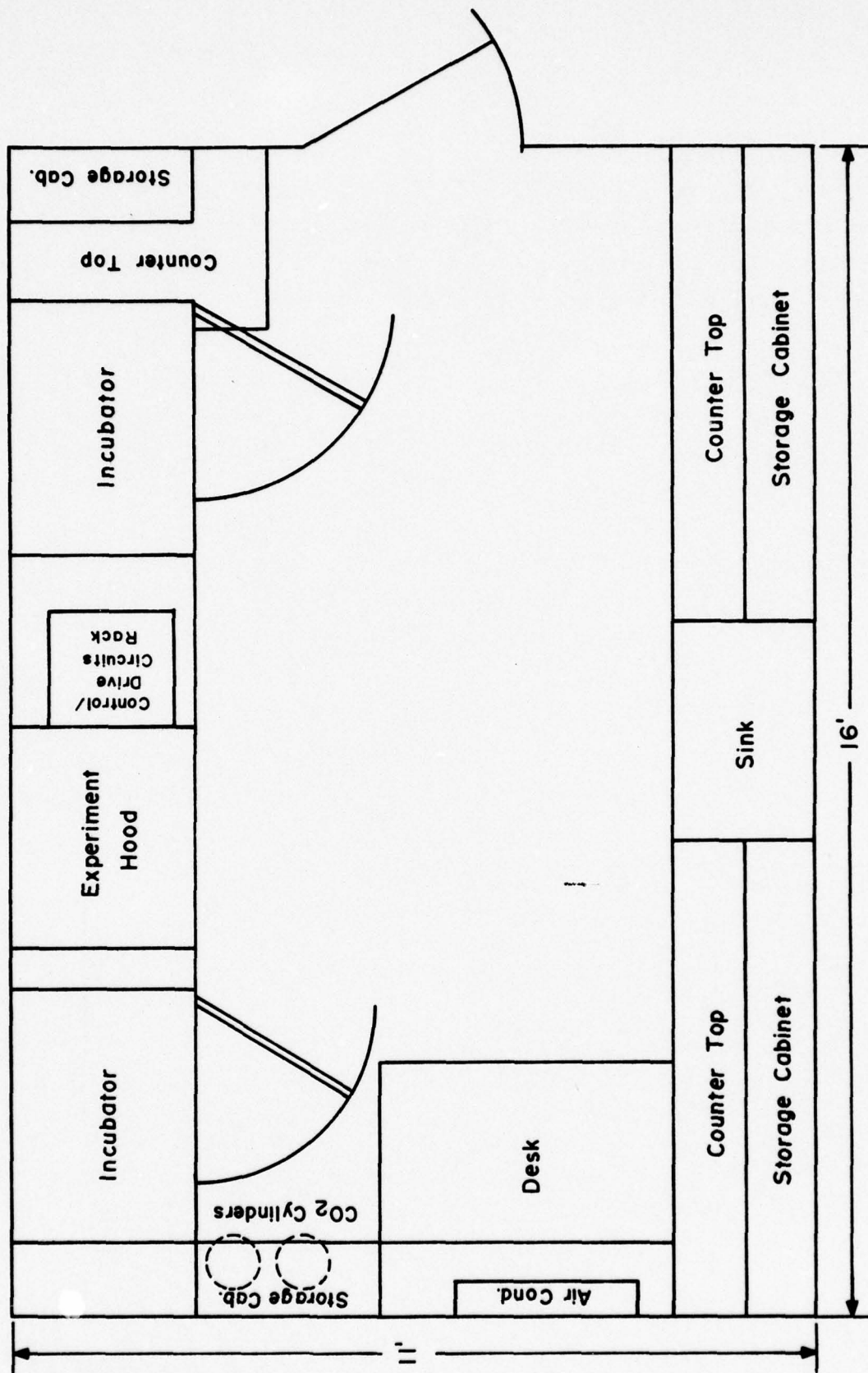


Fig. 15
LAYOUT OF ELF EXPOSURE, ROOM 115 - NMR

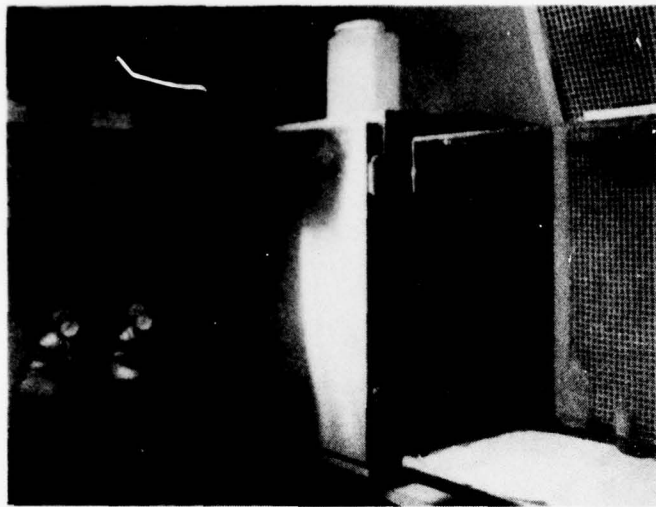
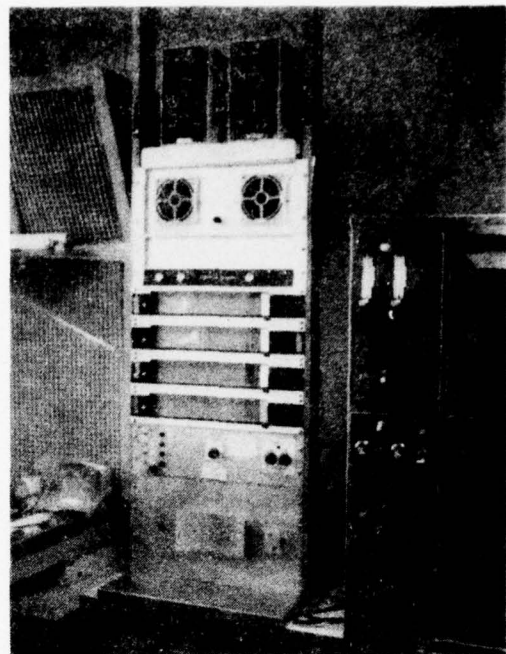


Figure 16a INCUBATOR, CO₂ TANKS, AND EXPERIMENTAL HOOD



Figures 16c (above) and d (below)
SIMULATED CONTROL, DRIVE,
AND MONITORING EQUIPMENT

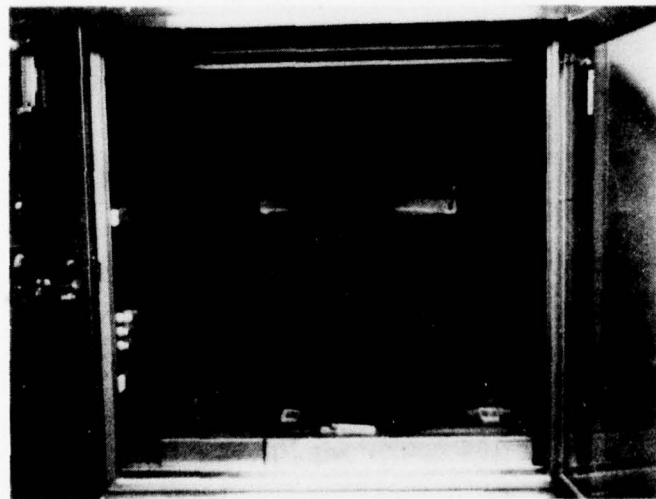
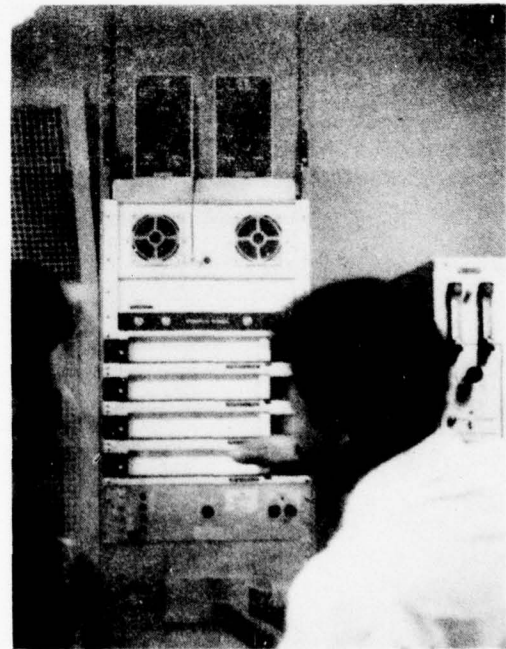


Figure 16b ELF ELECTROMAGNETIC FIELD SIMULATOR INSTALLED IN AN INCUBATOR



The ELF exposure room was air conditioned by a window unit installed over the desk. Lighting was provided by ceiling mounted fluorescent fixtures. An additional ceiling fixture contained an ultraviolet lamp to aid in maintaining sterile conditions in the room. The lamp was controlled by an interlock switch on the exposure room door for the safety of anyone entering the room.

3.2 Electromagnetic Field Measurements

3.2.1 Equipment and Methods

The sensors used for measuring the high impedance electric fields and the magnetic fields generated by the simulators were the IITRI-fabricated high impedance electric field probe⁸ and magnetic field probes. The electric field probe consists of a spherical sensor/transmitter, a fiber optic data link, and a receiver. The magnetic field probes are simply many turned coils of wire with ferrite cores and appropriate terminating resistors for flat frequency response. All the probes are sensitive on a single axis and produce an output voltage proportional to the field being measured. Figure 17 is a photograph of a magnetic field probe and the high impedance electric field probe. The magnetic field probe pictured was specially constructed to fit between the six-inch separation of the simulators' electric field plates. The plastic probe stands were designed to position the probes midway between the plates.

The meter used to measure the probes' output voltages was a Hewlett-Packard 3581A signal wave analyzer. The HP3581A functions as a frequency selective voltmeter, with factory modifications for battery and 1 Hz bandwidth operation. For these data, the HP3581A was used with a 1 Hz or 3 Hz bandwidth setting as required. Conversion tables were used to calculate the equivalent electric and magnetic field levels from the measured output voltages.

As no method had been devised at the time of the simulator installation to measure an MSK signal switching between 72 Hz and 80 Hz in the presence of 60 Hz ambient signals, a continuous sinusoidal (CW) signal of 76 Hz, the MSK center frequency, was used to drive the simulator from these measurements. This was done by temporarily replacing the MSK generator with a Tektronix FG501 function generator and DC503 counter supplied by NMRI. As the load

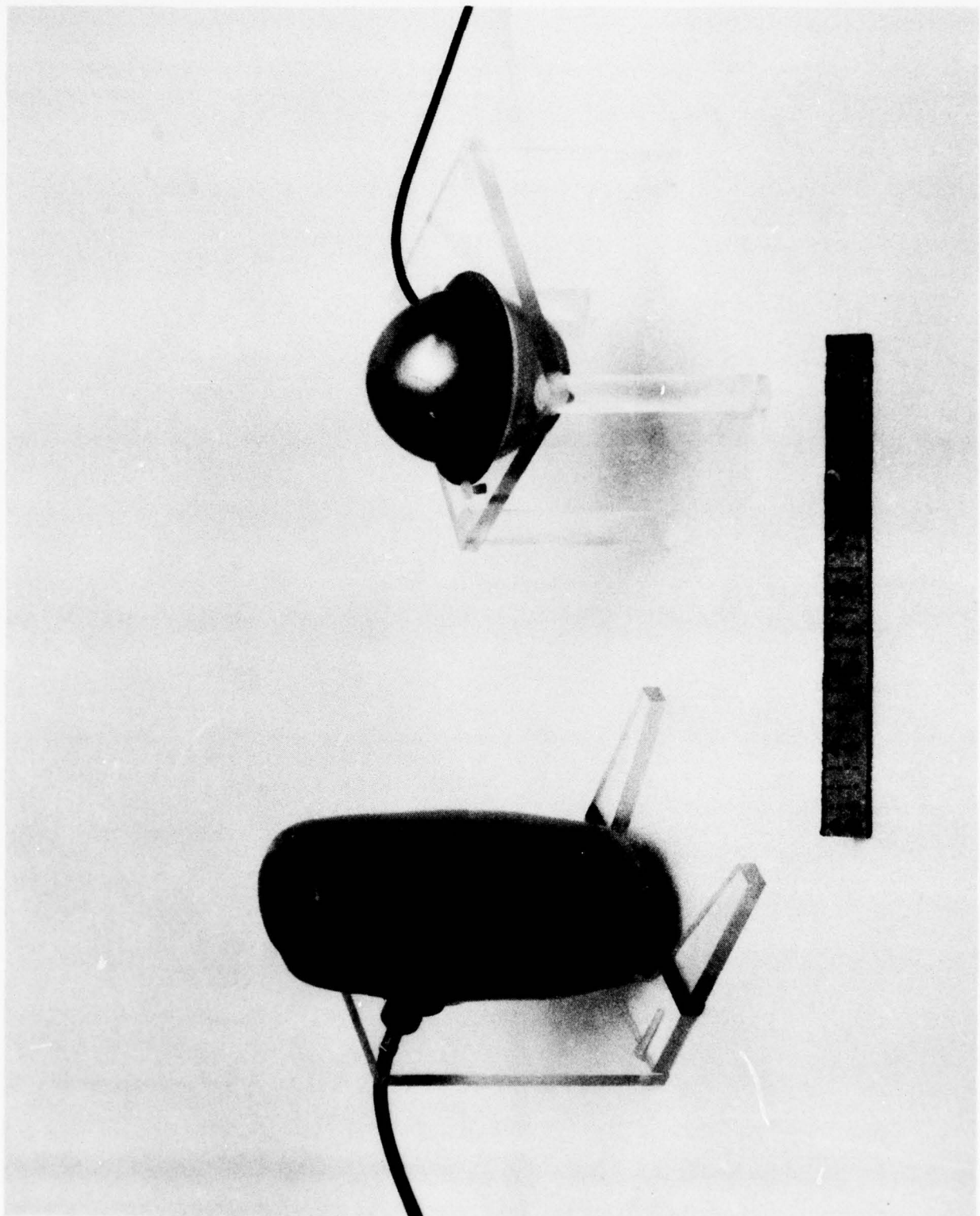


Figure 17 MAGNETIC FIELD PROBE (LEFT) AND HIGH IMPEDANCE ELECTRIC FIELD PROBE (RIGHT) WITH PLEXIGLASS STANDS

seen by the Crown drive amplifier was essentially constant over the 72-80 Hz frequency range, the field levels generated at 76 Hz were the same as those generated by the MSK signal. This measurement method allowed the HP3581A to discriminate between the generated field levels at 76 Hz and the ambient field levels at 60 Hz.

The ambient and simulator generated electric and magnetic fields were measured at numerous locations both inside and outside the incubators. At each test point three perpendicular components of each field were measured, and the corresponding field magnitudes were calculated as the square root of the sum of the squares of the field components. A diagram of the test points inside the incubators is shown in Figure 18, with dimensions referenced to the center of the electric field plates. The test point numbering scheme and orientation of the axis of measurement are also given.

3.2.2 Generated Field Inside the Incubator

Measurements of the 76 Hz simulator generated electric field intensity and magnetic flux density inside incubator A are presented in Table 1. These data show the degree of uniformity of the electromagnetic fields in the test volume of the simulator. The variation of the electric field intensity is shown to be about 7% for both the main (vertical) component and the magnitude of the field. The secondary field component (parallel and perpendicular) are at least an order of magnitude less than the main component. For the magnetic flux density, the variation from the value at the center position is seen to be less than \pm 7% with one exception for both the main (parallel) component and the magnitude. Likewise, the secondary field components (perpendicular and vertical) are typically at least two orders of magnitude below the main field component. For these measurements, the simulator was driven with a coil current of 41 mA and a plate potential of 3.65 volts. The generated EM fields in simulator B were not measured as the construction of the two incubators and the two simulators were identical for all practical purposes, and the field uniformity in simulator B should be very close to that in Simulator A.

3.2.3 60 Hz Ambient Fields

Sixty Hertz ambient electromagnetic fields are due to the presence of 60 Hz commercial electric power wiring and the equipments which operate from it. In particular, ambient electric fields tend to be generated by fluorescent

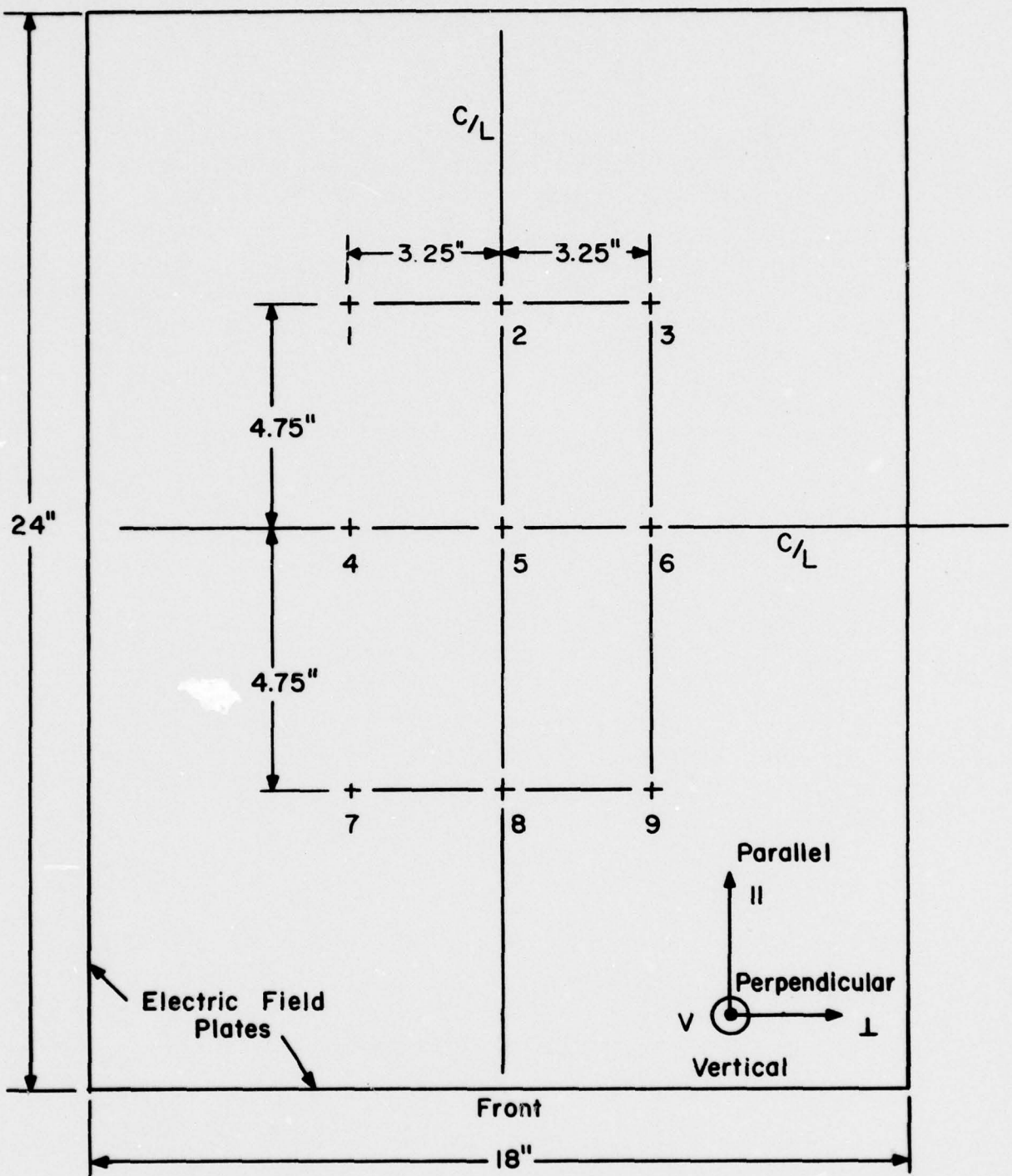


Fig. 18

TABLE 1
SIMULATOR GENERATED 76 Hz ELECTRIC FIELD INTENSITY (E) AND MAGNETIC FLUX DENSITY (B)
INSIDE INCUBATOR "A"

Position	$E_{ }$ V/m	E_{\perp} V/m	E_V V/m	$ E $ V/m	$B_{ }$ gauss	B_{\perp} gauss	B_V gauss	$ B $ gauss
1	0.48	0.47	14	14	0.15	0.0076	0.0036	0.15
2	0.57	0.35	14	14	0.15	0.0013	0.0049	0.15
3	0.54	0.69	14	14	0.15	0.0024	0.0044	0.15
4	0.14	0.42	15	15	0.17	0.0074	0.0029	0.17
5	0.10	0.29	15	15	0.16	0.0051	0.0061	0.16
6	0.25	0.84	15	15	0.16	0.0011	0.0034	0.16
7	0.26	0.38	15	15	0.14	0.020	0.0025	0.15
8	0.06	0.05	15	15	0.14	0.0002	0.0018	0.14
9	0.07	1.15	15	15	0.15	0.013	0.0013	0.15

NOTE: Coil current = 41 mA.

Plate Voltage = 3.64 volts.

lighting, electric wiring and cords, and other non-shielded electrical apparatus. Ambient magnetic fields are generated to some degree by wiring, but are more likely to be produced by fluorescent light ballast transformers, electric motors, and equipment containing electric motors and transformers. Several measurements were made outside of the incubators in room 115 to determine the ambient field levels present. These data were taken with the room fluorescent lights, the air conditioner, and the incubators operating. The ambient electric field at the center of the room, three feet above floor level, was on the order of 4 volts/meter. The ambient magnetic field at room center and over the desk was 0.0005 gauss or less.

The ambient electric and magnetic fields were also measured inside the incubators. These data are given in Table 2. Sixty hertz noise that coupled into the simulator drive cables set up 60 Hz ambient electric fields between the grounded incubator case and the electric field plates and magnetic field coils. The coupling was most severe for the non-driven control simulator. The coupling was significantly reduced by installing a shield on the drive leads; the shield was connected to the incubator case. Further reduction of the ambient electric fields in the control simulator was realized by shorting the electric field plates together and to the incubator case. As seen from Table 2, the magnitudes of the 60 Hz ambient electric fields in the simulators were on the order of 0.1 volt/meter. Slightly higher levels were measured in the control simulator, and slightly lower levels were measured in the test simulator. It was found that the ambient electric field levels could be reduced to 0.01 volt/meter in the control simulator by also grounding one side of the magnetic field coils to the incubator case.

The 60 Hz ambient magnetic field levels measured in the incubators were up to an order of magnitude higher than those measured in the room center. This was most likely due to the presence of a fan motor in the left wall of the incubator. Support for this theory is given by the increasing value of ambient magnetic field measured at the leftmost as compared to the rightmost test points, and by the similar behavior shown by both the test and control incubators. More than half of the test points had ambient magnetic fields less than or equal to 0.002 gauss, and all measured ambient fields were under 0.005 gauss.

TABLE 2
60 Hz AMBIENT ELECTRIC FIELD INTENSITY AND MAGNETIC FLUX DENSITY INSIDE INCUBATORS A & B

Simulator/ Position	$E_{ }$ V/m	E_{\perp} V/m	E_V V/m	$ E $ V/m	$B_{ }$ gauss	B_{\perp} gauss	B_V gauss	$ B $ gauss
A-1	0.070	0.014	0.026	0.076	0.0013	0.0031	0.0006	0.0034
A-2	0.084	0.030	0.020	0.091	0.0008	0.0017	0.0003	0.0019
A-3	0.070	0.055	0.031	0.095	0.0004	0.0014	0.0003	0.0015
A-4	0.011	0.027	0.020	0.035	0.0003	0.0044	0.0004	0.0044
A-5	0.005	0.005	0.020	0.022	0.0002	0.0024	0.0003	0.0024
A-6	0.0007	0.050	0.019	0.054	0.0003	0.0014	0.0003	0.0014
A-7	0.003	0.030	0.019	0.035	0.0019	0.0024	0.0003	0.0031
A-8	0.001	0.003	0.024	0.025	0.0010	0.0017	0.0003	0.0019
A-9	0.016	0.057	0.012	0.060	0.0006	0.0010	0.0003	0.0012
B-1	0.015	0.10	0.019	0.10	0.0021	0.0037	0.0004	0.0043
B-2	0.007	0.002	0.005	0.009	0.0011	0.0017	0.0002	0.0020
B-3	0.026	0.18	0.022	0.18	0.0006	0.0011	0.0003	0.0013
B-4	0.008	0.14	0.022	0.14	0.0003	0.0047	0.0002	0.0048
B-5	0.003	0.011	0.007	0.013	0.0004	0.0027	0.0003	0.0027
B-6	0.014	0.26	0.036	0.26	0.0002	0.0018	0.0003	0.0019
B-7	0.007	0.092	0.018	0.094	0.0021	0.0025	0.0001	0.0032
B-8	0.047	0.092	0.010	0.10	0.0007	0.0013	0.0001	0.0015
B-9	0.30	0.46	0.069	0.56	0.0002	0.0003	0.0004	0.0009

NOTES:

Simulator A driven; coil current = 41 mA, plate voltage = 3.65
Simulator B not connected, plates shorted to incubator case.
Incubators, Room Lights, and Air Conditioner on.

3.2.4 Cross-Coupling of Simulator Generated Fields

Table 3 presents data on the coupling of electromagnetic fields from a test simulator to a control simulator. Measurements were made in simulator B, with simulator A driven at three different field levels. As shown by the data, the maximum cross-coupled magnetic field, with simulator A driven at nearly 8 gauss, was on the same order as the ambient magnetic field in the simulators. The cross-coupled electric field was so low as to be in the output noise level of the electric field probe receiver, about 0.002 volt/meter. This is nearly two orders of magnitude below the average ambient electric field levels.

3.2.5 Simulator Generated External Fields

To determine to what extent laboratory personnel might be exposed to the simulator generated electric and magnetic fields, a series of measurements at various work stations in room 115 were made. Simulator A was driven at two different magnetic field levels. The results are given in Table 4. Six inches in front of the incubators, the magnetic field is reduced by only a factor of five, while the electric field is barely measurable at 0.004 volt/meter. At distances of two feet or more from the incubators, however, the magnetic field is reduced by at least two orders of magnitude. These generated magnetic field levels, although somewhat higher than the ambient magnetic field levels present in the room, are typical of those that might be encountered near many common, small household appliances such as can openers or mixers. A list of comparative electromagnetic environments is given in Tables 5 and 6.

TABLE 3
SIMULATOR CROSS-COUPING AT 76 Hz

Simulator A		Simulator B			
		B_1 gauss	B_V gauss	$ B $ gauss	$ E_1 $ V/m
0.157	0.00011	<0.00001	<0.00011	0.00011	<0.0015
0.787	0.00058	0.00004	0.00001	0.00059	<0.0013
7.75	0.00562	0.00056	0.00020	0.00565	<0.0013

NOTE:
Simulator A Plate Volts = 3.64
Simulator B not connected, plates shorted to ground.

TABLE 4
76 Hz SIMULATOR GENERATED MAGNETIC FLUX DENSITIES OUTSIDE THE INCUBATORS

Magnetic Flux Density Inside Simulator A gauss	$B_{ }$ gauss	B_{\perp} gauss	B_V gauss	$ B $ gauss	Location of Measurement
7.75	1.24	0.135	0.067	1.25	6" in front of incubator A
7.75	0.054	0.074	0.022	0.094	24" from A in experiment hood
7.75	0.052	0.021	0.040	0.067	30" from A over desk
7.75	0.002	0.017	0.009	0.019	3' high at room center
0.157	0.0247	0.0045	0.0025	0.0252	6" in front of incubator A
0.157	0.0015	0.0016	0.0004	0.0022	24" from A in experiment hood
0.157	0.0012	0.0006	0.0011	0.0018	30" from A over desk
0.157	<0.0001	0.0002	0.0001	0.0003	3' high at room center

NOTE: Simulator A Plate Volts = 3.65

TABLE 5
60 Hz EM FIELDS NEAR ELECTRICAL APPLIANCES/DEVICES

Appliance/Device	E (V/m)	B (Gauss)	Measurement Location
Electric Dryer	1.3	0.0037	30 cm from front, 1 m high
Washer	5.8	0.0043	30 cm above top near front
Radial Arm Saw	8.6	0.268	30 cm in front of
Dehumidifier	2.4	0.0020	30 cm away
Soldering Gun	119.	0.244	30 cm away
Bench Grinder	9.6	0.183	30 cm away (front)
Hand Drill	260.	0.183	15 cm away
Electric Coffee Pot	30.	0.0009	30 cm away
Incandescent Light	2.0	0.0008*	15 cm away
Hand Held Hair Dryer	202.	0.0030	15 cm away
Range Hood	77.	0.0037*	30 cm away
20" Box Fan	112.	0.0037*	30 cm in front of
Electric Broiler	130.	0.091 0.028	30 cm above 30 cm in front of
Clock Radio	15.	0.0098	30 cm away
Upright Vacuum Cleaner	16. --	0.366 0.029	30 cm above motor 30 cm behind, 1 m high
Iron	60. --	0.0023* 0.024	30 cm from handle 7 cm from handle
TV (color)	30.	0.0091	30 cm in front

* ambient (room ambient level).

--- No measurement made.

TABLE 5 (Cont.)
60 Hz EM FIELDS NEAR ELECTRICAL APPLIANCES/DEVICES

Appliance/Device	E (V/m)	B (Gauss)	Measurement Location
Stereo Power Amplifier	90.	0.012	30 cm above
Toaster	40.	0.012	30 cm from side
Refrigerator	60.	0.0016	30 cm away, 1 m high
Hand Mixer	50.	3.4	15 cm from handle
Fluorescent Ceiling Light (round)	4.8	0.0022	1.75 m above floor .75 m from light
Garbage Disposal	1.8	0.037	30 cm away
Electric Stove	0.76	0.055	30 cm above front burner
Electric Oven	1.5	0.0043	30 cm from front, 1 m high
Dishwasher	2.7	0.0085	30 cm from front, 1 m high
Can Opener	68.	0.171	30 cm away

TABLE 6
60 Hz EM FIELDS IN THE CENTER OF VARIOUS ROOMS IN A TYPICAL HOME

Location	E (V/m)	B (Gauss)
Kitchen	3.0	0.0004
Kitchen	---	0.0023
Laundry/Basement	1.0	0.0018
Work Area/Laundry	1.2	0.0020
Yard	0.33	0.0012
Shop	---	0.0055
Recreation Room	---	0.0007

--- Measurement not made.

REFERENCES

1. S. M. Michaelson, "Human Exposure to Nonionizing Radiant Energy - Potential Hazards and Safety Standards," Proceedings of the IEEE, 60 (April 1972), 389-421.
2. M. H. Benedick and B. Greenberg, "The Sanguine Biological-Ecological Research Program," IEEE Transactions on Communications, COM-22(4) (April 1974).
3. United States Navy, Electronic Systems Command, "Appendix E: Biological and Ecological Information," Seafarer ELF Communications System Draft Environmental Impact Statement for Site Selection and Test Operations (Washington, D. C., February 1977).
4. "Biological Effects of High Voltage Electric Fields," Electric Power Research Institute Final Report EPRI 281-1 (November 1975).
5. Y. Shiau, "ELF Electric Field Analysis for a Laboratory Biological Experiment," IIT Research Institute Technical Report E6357-9 (December 1977).
6. S. Ramo, J. Whinnery, and T. Van Duzen, Fields And Waves In Communications Electronics (New York: John Wiley & Sons, 1967), 108-111.
7. V. C. Formanek and J. R. Gauger, "Design and Operation of a Minimum Shift Keying (MSK) Generator," IIT Research Institute Technical Report E6249-1 (first revision, May 1977).
8. V. C. Formanek, "An Improved ELF Electric Field Probe," IIT Research Institute Technical Memorandum E6249-2 (March 1974).

APPENDIX A
DESIGN OF A MULTI-COIL MAGNETIC FIELD SIMULATOR

The basic design requirement of a magnetic field simulator for use in biological-ecological experimentation is that it must produce a uniform magnetic field over a desired test volume. Variation of the field within the volume should not be more than about 10%. For a multi-coil magnetic field simulator, the first steps in the design are to determine a) how many coils are needed, b) what radius/spacing ratio is required, and c) how many relative turns/coil should be used to optimize the uniformity of the magnetic field inside the simulator.

The obvious first try is to use Helmholtz coils with the spacing equal to the radius, since it can be shown that such a configuration provides an especially uniform field near the center. In order to determine how large the coils must be to obtain the desired field uniformity within the required test volume, the variation of the field away from the axis must be known. However, the expressions for determining the magnetic field at points other than along the coil axis are not readily available in literature. Therefore, the first step in the analysis is the derivation of the general expressions for the quasi-static magnetic field for a circular loop.

The magnetic vector potential for a circular loop of radius a is given by the following equation¹ for the cylindrical coordinate system shown in Figure 1:

$$A_\phi = \frac{\mu_0 I a}{\pi \sqrt{a^2 + z^2 + \rho^2 + 2ap}} \left[\frac{(2 - k^2)K(k) - 2E(k)}{k^2} \right] \quad (1)$$

where

$$k^2 = \frac{4ap}{a^2 + z^2 + \rho^2 + 2ap} \quad (2)$$

$K(k)$ = complete elliptic integral of the first kind

$E(k)$ = complete elliptic integral of the second kind.

The magnetic induction is given by

$$\vec{B} = \nabla \times \vec{A} \quad (3)$$

which reduces to

$$\vec{B} = B_\rho \vec{I}_\rho + B_z \vec{I}_z \quad (4)$$

where

$$B_\rho = \frac{\partial \phi}{\partial \rho} \quad (5)$$

and

$$B_z = \frac{1}{\rho} \frac{\partial(\rho A\phi)}{\partial \rho} \quad (6)$$

Using Equations 1, 5 and 6 it can be shown that

$$B_\rho = \left[\frac{\mu_0 I a}{\pi} \right] \left[\frac{m^3 z}{(1-k^2)} \right] \left[K(k) - (2-k^2) D(k) \right] \quad (7)$$

and

$$B_z = \left[\frac{\mu_0 I}{4\pi} \right] \left[\frac{m}{(1-k^2)} \right] \left[4a^2 m^2 E(k) + k^2 (2-k^2) D(k) - k^2 K(k) \right] \quad (8)$$

where

$$m = \frac{1}{\sqrt{a^2 + z^2 + \rho^2 + 2a\rho}} \quad (9)$$

$$k = 2 \sqrt{\frac{ap}{a^2 + z^2 + \rho^2 + 2a\rho}} \quad (10)$$

$K(k)$ = Complete elliptic integral of the first kind

$$= \frac{\pi}{2} \left\{ 1 + \left(\frac{1}{2} \right)^2 k^2 + \left(\frac{1 \cdot 3}{2 \cdot 4} \right)^2 k^4 + \dots + \left[\frac{(2n-1)!!}{2^n \cdot n!} \right]^2 k^{2n} + \dots \right\} \quad (11)$$

$E(k)$ = Complete elliptic integral of the second kind

$$= \frac{\pi}{2} \left\{ 1 - \frac{1}{2^2} k^2 - \frac{1^2 \cdot 3}{2^2 \cdot 4^2} k^4 - \dots - \left[\frac{(2n-1)!!}{2^n \cdot n!} \right]^2 \frac{k^{2n}}{(2n-1)} - \dots \right\} \quad (12)$$

$$\begin{aligned}
 D(k) &= \frac{K(k) - E(k)}{k^2} \\
 &= \pi \left\{ \frac{1}{1} \left(\frac{1}{2} \right)^2 + \frac{2}{3} \left(\frac{1 \cdot 3}{2 \cdot 4} \right)^2 k^2 + \dots + \frac{n}{2n-1} \left[\frac{(2n-1)!!}{2^n \cdot n!} \right]^2 k^{2(n-1)} + \dots \right\} \quad (13)
 \end{aligned}$$

Equations 7 through 13 can be used to determine the quasi-static magnetic field due to a circular loop of radius a located as shown in Figure A-1. Further, by means of coordinate translation and super-position, these equations can be used to calculate the magnetic field at any point due to any number of coaxial loops. Therefore, these equations were programmed and used to theoretically determine the field variation of various coil configurations. A listing of the FORTRAN IV computer program used to calculate the off-axis magnetic field due to a number of coaxial coils is given in Table A-1.

Based on the theoretical analysis, it was determined that a three-coil configuration, with spacing equal to half the radius, N turns on the center coil, and $2N$ turns on the end coil, would yield the desired field uniformity over a larger volume than a set of Helmholtz coils, where the spacing equals the radius. In order to verify these results, a three-coil configuration was constructed. It had a radius of two feet and a coil spacing of one foot. Each of the end coils had 236 turns of wire while the center coil had 118 turns of wire. This configuration was designed to produce a one-gauss magnetic flux density with the coils connected in series and a coil current of 213 mA.

The first test performed was to adjust the current through the simulator to 213 mA and measure the magnetic field at the center. The measured magnetic flux density at the center was 1.0 gauss as predicted.

The next test performed was to measure the magnetic field variation of the simulator for comparison with the theoretically predicted variation. The current through the simulator was adjusted so that the magnetic field at the center was 5 gauss ($I = 1.06$ amps) and the magnetic field was measured at the following locations (see Figure A-2 for the reference coordinate system):

- At 2 inch intervals along the z -axis ($\rho = 0$)
- At 2 inch intervals along a radial in the plane of the center coil ($z = 0$).

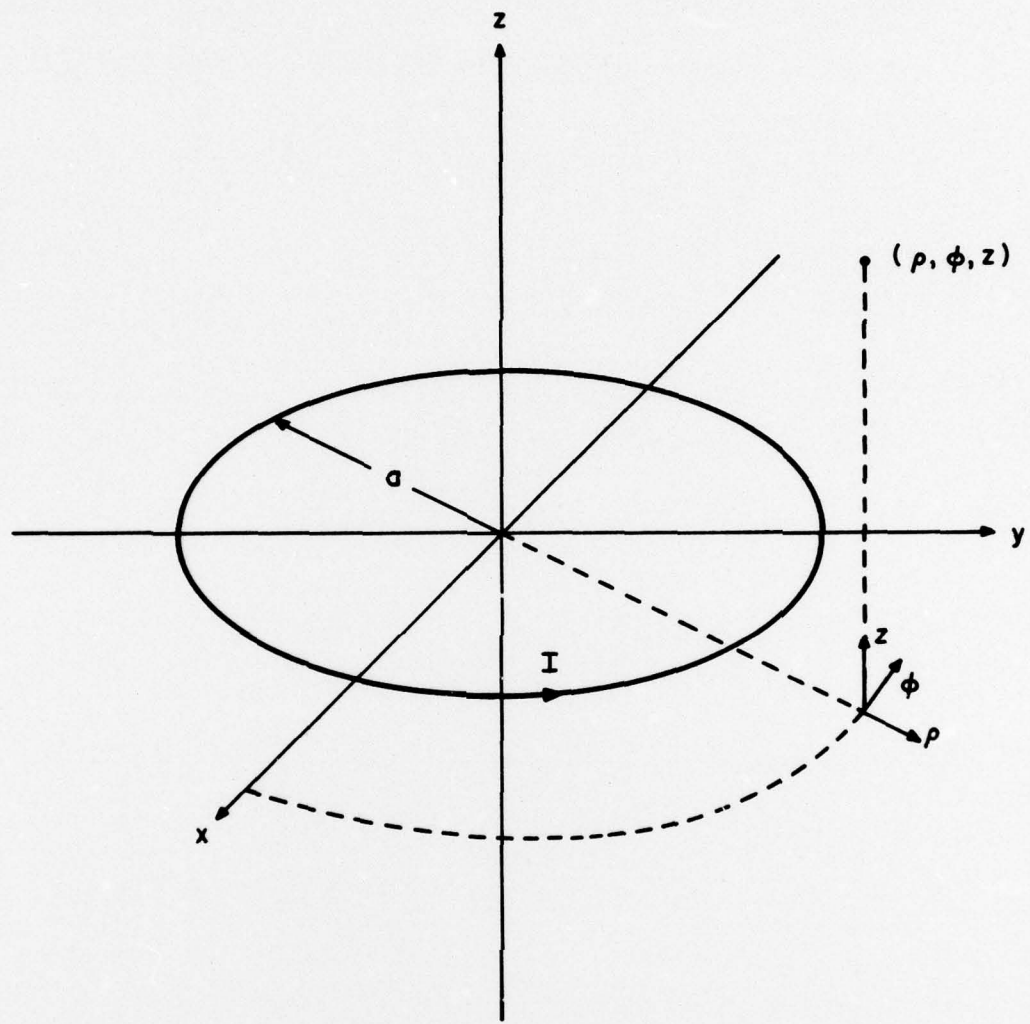


Fig. A-1

CYLINDRICAL COORDINATE SYSTEM FOR A CIRCULAR LOOP

TABLE A-1

LISTING OF FORTRAN IV COMPUTER PROGRAM TO CALCULATE THE OFF-AXIS
B-FIELD DUE TO MULTIPLE COAXIAL COILS

```

1 DIMENSION BR(10),BZ(10)
2 REAL N,M,K,KK
4 PI=4.*ATAN(1.)
6 U=4.*PI*1.E-7
8 A=2.0*0.3048
10 H=1.0*0.3048
12 CUR=1.0
14 1 WRITE (6,100)
16 READ(5,*)RR,ZZ
17 R=RR*2.54E-02
18 IF (R.EQ.10.0) STOP
19 Z=ZZ*2.54E-02
20 Z1=Z-H
22 Z2=Z+H
24 Z3=Z
25 DO 26 II=1,3
26 IF (II.LT.3) CUR=1.0
27 IF (II.EQ.3) CUR=0.5
30 IF(II.EQ.1)Z=Z1
35 IF(II.EQ.2)Z=Z2
36 IF (II.EQ.3) Z=Z3
40 M=1./SORT(A**2+Z**2+R**2+2.*A*R)
45 K=2.*SORT(A*R/(A**2+Z**2+R**2+2.*A*R))
50 SUM=0.0
60 D=1.0
70 DO 20 I=1,500
80 N=FLOAT(I)
90 SUM=SUM*D
100 D=D*((2.*N-1)/(2.*N))**2*K**2
110 IF (ABS(D/SUM).LT.0.0001) GO TO 21
120 20 CONTINUE
130 21 SUM=SUM+D
140 KK=PI/2.*SUM
150 SUM=2.
160 B=1.0
170 DO 22 I=1,500
180 N=FLOAT(I)
190 SUM=SUM-B
200 B=B*((2.*N-1)/(2.*N))**2*K**2/(2.*N-1.)*ABS(2.*N-3.)
210 IF (ABS(B/SUM).LT.0.0001) GO TO 23
220 22 CONTINUE
230 23 SUM=SUM-B
240 EK=PI/2.*SUM
250 SUM=0.0
260 C=(1./2.)**2

```

TABLE A-1 (Cont.)

```

270 DO 24 I=2,500
280 N=FLOAT(I)
290 SUM=SUM+C
300 C=C*((2.*N-3.)/(N-1.))*(N/(2.*N-1.))*((2.*N-1.)/(2.*N))**2%
301 *K**2
310 IF (ABS(C/SUM).LT.0.0001) GO TO 25
320 24 CONTINUE
330 25 SUM=SUM+C
340 DK=PI*SUM
350 BR(II)=(U*CUR*A/PI)*(M**3.Z/(1.-K**2))*%
351 (KK-(2.-K**2)*DK)
360 BZ(II)=(U*CUR/(4.*PI))*(M/(1.-K**2))*%
361 (4.*A**2*M**2*EK+K**2*(2.-K**2)*DK-K**2*KK)
370 26 CONTINUE
380 BRR=0.0
390 BZZ=0.0400 DO 27 II=1,3
410 BRR=BRR+BR(II)
420 27 BZZ=BZZ:BZ(II)
430 B=SQRT(BRR**2+BZZ**2)
440 THETA=ATAN2(BRR,BZZ)
445 Z=Z3
446 B=B*236.*0.213*1.E+04
447 BRR =BRR*236.*0.213*1.E+04
448 BZZ-BZZ*236.*0.213*1.E+04
450 WRITE (6,101) RR,ZZ,B,THETA,BRR,BZZ
460 GO TO 1
470 100 FORMAT(' R=?      Z=?')
480 101 FORMAT(1P6E10.2)
490 STOP
500 END

```

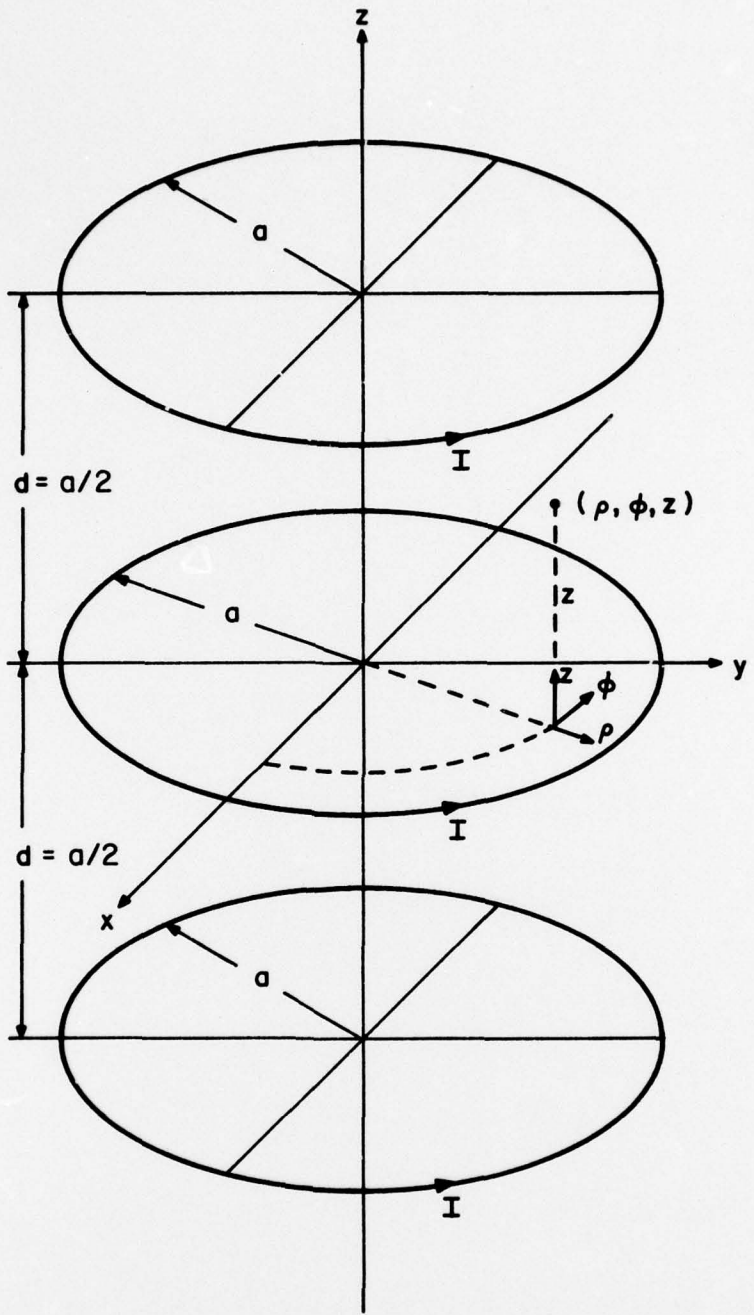


Fig. A-2

COORDINATE SYSTEM FOR THE THREE COIL CONFIGURATION

These experimental results were normalized to one gauss and are plotted in Figures A-3 and A-4 for comparison with the theoretically predicted fields. The theoretically predicted fields were calculated using the previously described computer program, which is based on Equations 7 through 13. As shown in the figures, there is excellent agreement between the theoretical and experimental results.

REFERENCE

1. J. D. Jackson, Classical Electrodynamics. (New York: John Wiley & Sons, 1962), pp. 141-142.

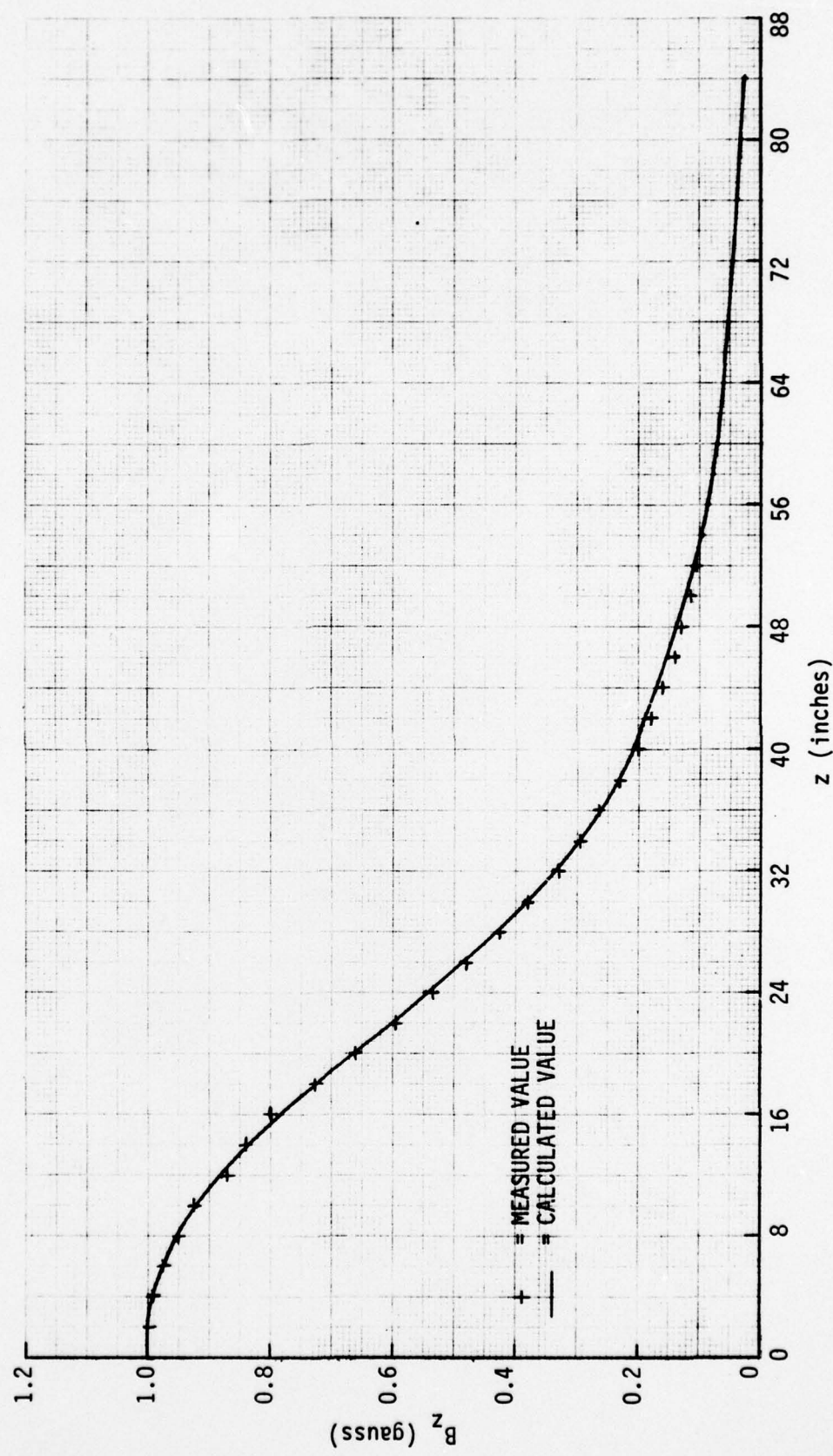


Figure A-3 COMPARISON OF THE MEASURED AND CALCULATED MAGNETIC FLUX DENSITY ALONG THE SIMULATOR AXIS ($\rho = 0$)

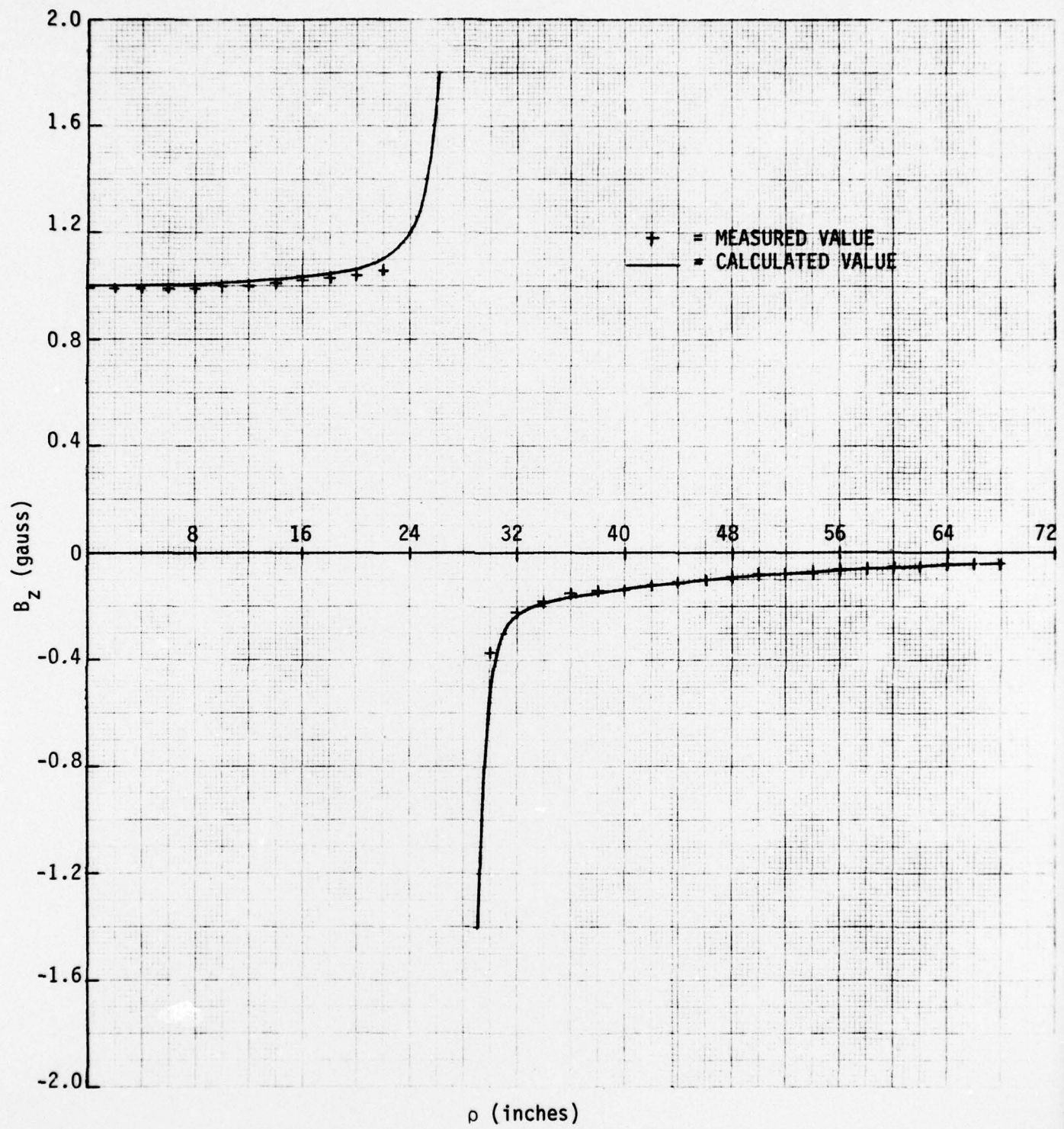


Figure A-4 COMPARISON OF THE MEASURED AND CALCULATED MAGNETIC FLUX DENSITY VERSUS PERPENDICULAR DISTANCE FROM THE SIMULATOR AXIS AT $z = 0$

Unclassified

SECURITY CLASSIFICATION OF THIS PAGE (When Data Entered)